Shallow-Marine Tidal Deposits

13

Jean-Yves Reynaud and Robert W. Dalrymple

Abstract

Shallow-marine tidal deposits form on open shelves, and more specifically in open-mouthed embayments and semi-enclosed epicontinental seas, where the oceanic tide is amplified by resonance. They are also present in straits and seaways where the tidal currents are accelerated by flow constriction. Complex interactions of the tide with the seafloor and coastal topography bring about tidal asymmetry, generating tidal-transport pathways with net, unidirectional transport of sediment over long distances. Tidal currents are commonly capable of resuspending mud in shallow-marine settings, but little is known about the role of tidal currents in the deposition of muddy deposits in the offshore domain. The best-known shelf tidal deposits are sandy and bioclastic transgressive 'lags' that mantle flooding surfaces. These lags are generally thin, but can reach thicknesses of 10–30 m in tidal-current ridges and sand sheets. These deposits are composed of dominantly well-sorted, cross-bedded sands with good reservoir properties. Careful architectural analysis allows the distinction between the deposits of compound dunes, tidal-current ridges and migrating sand sheets. The occurrence of shallow-marine tidal deposits is sensitive to changes in sea level; paleotidal modeling has great potential to help understanding their occurrence in space and time.

13.1 Introduction

Shallow-marine areas, which includes continental shelves and shallow-water seas, are considered here to extend from near the coast to the shelf break, spanning water depths from as shallow as 10–20 m to as much as 150–200 m, and up to 400 m along some formerly glaciated margins. The tides, which generally are created in the open ocean, pass over the shelf on their way to the coast, interacting with the seafloor as they go (Wright et al. 1999; Allen 1997). Geomorphologically, continental shelves and shallow-water seas are diverse. Most continental shelves with significant tidal currents occur on wide passive continental margins, because tidal action typically increases as shelf width becomes greater. Such shelves are commonly straight, with the shoreline essentially parallel to the shelf break for several hundred kilometers. Structural complexities in continental margins create large-scale *embayments*,

J.-Y. Reynaud (✉)
Département Histoire de la Terre – UMR 7193 ISTeP,
Muséum National d'Histoire Naturelle, Géologie,
CP 48, 43, rue Buffon, F-75005 Paris, France
e-mail: jyr@mnhn.fr

R.W. Dalrymple
Department of Geological Sciences and Geological Engineering,
Queens University, Kingston, ON K7L 3N6, Canada
e-mail: dalrymple@geol.queensu.ca

R.A. Davis, Jr. and R.W. Dalrymple (eds.), *Principles of Tidal Sedimentology*,
DOI 10.1007/978-94-007-0123-6_13, © Springer Science+Business Media B.V. 2012

which are here defined as open-mouthed indentations of the coastline such as the North Sea and Yellow Sea. In such epicontinental embayments, the distance from the shoreline to the shelf margin can increase significantly and the flow is partially confined. Broad shallow-marine basins can also occur within continental interiors, far removed from a continental margin, with only a narrow and/or circuitous connection with the open ocean (e.g. Hudson Bay, Canada; the Baltic Sea). Such water bodies are termed semi-enclosed epicontinental seas here. Straits or seaways joining two larger bodies of water commonly exhibit particularly strong tidal water motions (e.g. the Strait of Dover in the English Channel). In all of these offshore settings, currents generated by the tides interact with an array of other processes, including waves, storm/wind-generated currents and geostrophic currents that are part of the global-ocean circulation, giving the potential for the creation of a complex variety of sedimentary deposits.

Because of the large geographic extent and substantial water depth of modern shallow-marine areas, our knowledge of the processes operating there, and of the sedimentary facies generated by these processes, has mostly been obtained by indirect observations. Our understanding of tidal dynamics on shelves has increased markedly over the last few decades, both as a result of improved instrumentation and the application of numerical-modeling approaches. Significant advances have also occurred in our ability to obtain detailed images of the sea floor (e.g. through the use of swath bathymetry), but high-quality 3D seismic imaging of subsurface deposits on modern shelves remains beyond the capability of most academic institutions. In addition, coring techniques have not evolved much over the last several decades; consequently, information on the nature of modern deposits is scanty, although the available database is increasing. As a result, facies models for the deposits of tidal shelves remain poorly developed, as reflected by most textbooks (Stride 1982; de Boer et al. 1988; Suter 2006).

This chapter begins by examining qualitatively some aspects of the dynamics of tides as they progress from the open ocean toward the coast. Then the range of deposits that can occur in tidal settings is considered, namely their composition, surficial morphology (i.e., the bedforms that are present) and internal structure. We focus on the origin and dynamic behavior of *compound dunes* (also called *sand waves*) and *tidal-current ridges* (also called *banks* and *bars*) because they are the largest and most distinctive of the tidally generated bedforms in shallow-marine settings. Reconstructing the Holocene evolution of the offshore ridges in various tidal basins helps to define a model for the transgressive evolution of these large sand bodies, which might have application to the rock record. Finally the potential response of shallow-marine tidal systems to physiographic changes caused by variations in relative sea level is examined briefly, taking examples from both the modern and the rock record. This is coupled with the insights gained from paleotidal modeling, in order to extend our understanding of where tidal deposits are likely to occur in time and space.

13.2 Tidal Processes In shallow Seas

The ability of a basin to develop a large tide depends on the possibility of an amphidromic system to be generated within the basin by the astronomic tide, and on water motions to be amplified by co-oscillation within the basin as the basin borders reflect the tidal wave (co-oscillating tide). The minimum size of a sea (a basin) where the tide is able to generate an amphidromic system is determined by the Rossby radius of deformation of the tidal wave (Pugh 1987), which is the minimum distance required for the Coriolis effect to cause a motion to rotate through 360° (Fig. 13.1a). The Rossby radius decreases as the Coriolis effect increases with increasing latitude. This implies that, for the same basin depth, amphidromic cells are smaller at higher latitude. Wave theory predicts an increase in the celerity of the tidal wave, and hence a larger Rossby radius, as water depth increases: because the perimeter of an amphidromic cell has to be traversed by the tidal wave within one tidal cycle, the larger the amphidromic cell, the higher the celerity the wave must have at its periphery. This is one reason why no shallow, semi-enclosed epeiric sea has significant tides, even though its dimensions are large enough to contain an amphidromic cell. This is, for example, the case in Hudson Bay or the Baltic Sea. Of course, semi-enclosed seas can have large tides even if they are not able to develop tides by themselves, as they can amplify an oceanic tide that enters them through a wide oceanic connection. This is the case in the North Sea and English Channel (Fig. 13.2).

Water motion associated with a rotating Kelvin wave involves two components: the main flow that is perpendicular to the crests and troughs of the wave (i.e., perpendicular to the cotidal lines that show the location of the wave crest as a function of time;

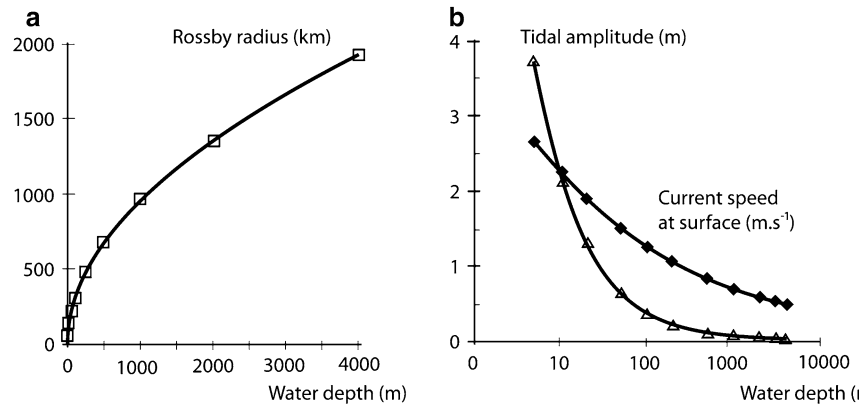

Fig. 13.1 (**a**) Rossby radius (i.e. the dimension of an amphidromic system) as a function of water depth. The Rossby radius is calculated as $R=[(g*d)^{1/2}]/f$ where g is the gravitational acceleration (9.81 m/s^2), d is the water depth and f is the Coriolis parameter (taken at 45° latitude: $10.3*10^{-5}$/s). Amphidromic systems in shallow water have a smaller diameter than those in the deep ocean. (**b**) Amplitude (half the tidal range) and related current velocity at the water surface for a 0.5 m-high, incident tidal wave as it shoals across a continental rise and shelf (see Allen 1997 for details). The relationship between Ad, the amplitude of the tide in deep water, As, its amplitude in shallow water, and Δd, the rate of the decrease in water depth, is expressed by $As=Ad(\Delta d)^{1/4}$. The speed of the surface current, U, is given by $U=A(gd)^{1/2}/d$. In nature, the tidal amplitude and related current velocity do not increase as much as is shown because of the influence of bottom friction (see Fig. 13.3)

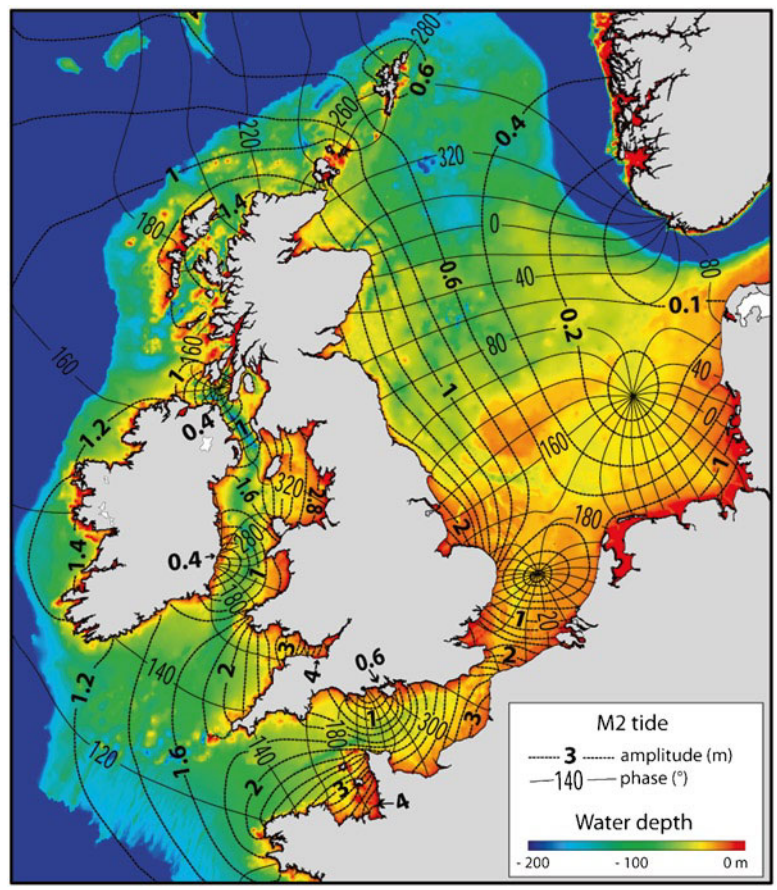

Fig. 13.2 Map showing the amphidromic systems in the seas surrounding the British Isles (After Sinha and Pingree 1997; bathymetry from GEBCO digital atlas, courtesy of Martin Wells). Only the M2 (principal lunar semi-diurnal tide) is considered. Cotidal lines are perpendicular to the coast, which means that the tidal wave travels parallel to the coast, creating tidal currents that are also coast-parallel. Further offshore (e.g. near the Atlantic continental margin), co-tidal (or phase) lines are nearly parallel to the shelf edge, bringing about currents perpendicular to the isobaths. The tidal range increases outward from each amphidromic point, with the highest tidal ranges within embayments such as the German Bight and The Wash, England

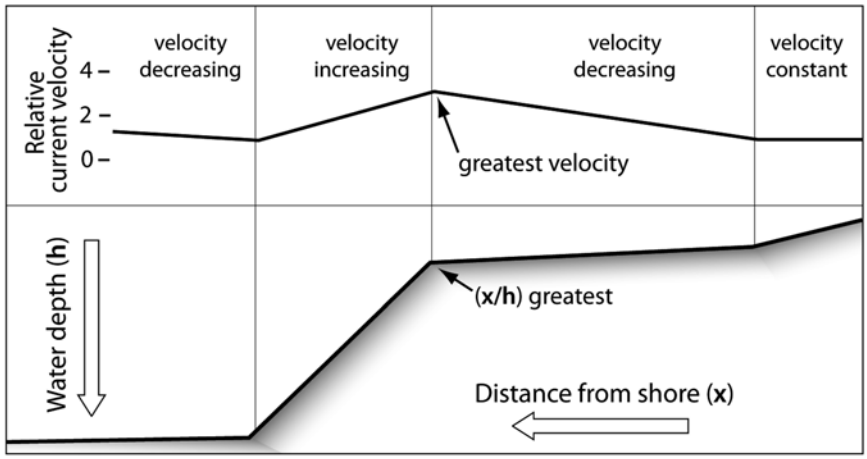

Fig. 13.3 Hypothetical distribution of depth-averaged current speed along a transect perpendicular to a shelf margin. As the tidal wave passes onto the shelf, reduction of the cross-sectional area creates an increase in the current speed. On the shelf, friction in shallow water reduces the tidal-current speed. The result is a zone of maximum current speed near the shelf edge (After Fleming and Revelle 1939)

Fig. 13.2), and a secondary flow that is parallel to the crests and troughs that results from the rotation of the tidal wave. As a consequence, the tidal-current direction at each point in an amphidromic system rotates over a tidal cycle, creating a *tidal ellipse* that traces out the path taken by the tip of successive current vectors. The fastest tidal currents in each tidal cycle (i.e. the major axis of the tidal ellipse) are nearly perpendicular to the co-tidal lines. The propagation direction of the tidal wave and the associated currents are essentially parallel the coast. In river mouths, by comparison, the tidal wave propagates up the river as a standing wave, so that the currents are approximately perpendicular to the nearby coast. On continental shelves, the peak flood and ebb currents are commonly not parallel, because the cotidal lines are not symmetrically distributed within each amphidromic cell, due to the unequal speed of migration of the incoming and outgoing tidal waves (Fig. 13.2).

Where the tide is channelized in a seaway that is much narrower than the radius of the amphidromic cell, the cotidal lines become nearly parallel with each other and are approximately perpendicular to the seaway axis. As a result, the amount of rotation of the currents decreases and they can even become rectilinear. This is the case for the English Channel: the tidal ellipses are greatly elongated and the peak currents are more or less parallel to the direction of travel of the tidal wave and essentially reverse by 180°.

13.2.1 Modification of the Oceanic Tide on the Shelf

The amplitude of the tide in deep oceanic waters is commonly less than 1 m. It increases and, consequently, tidal-current speeds increase, as water depth decreases at the continental margin. This is easily calculated with basic formulae of wave theory (Fig. 13.1b). However, as the tide progresses into shallower water further onto the shelf, frictional dissipation of tidal energy at the sea bed becomes important. Consequently, an area of maximum tidal-current speed is developed near the shelf edge (Fig. 13.3), largely because the tidal prism (i.e., the volume of water passing any point during each half tidal cycle) is greatest near there. The enhancement of tidal currents in this area may also be due to the presence of internal tides that occur along density interfaces in the ocean and break as they impinge on the continental slope (Legg and Adcroft 2003; see Chap. 14). Internal tides are generally important in a zone only a few tens of kilometers wide on the outer shelf and decrease in importance toward the coast. The best studied example is on the outer shelf of the Western Channel Approaches, seaward of the English Channel, where an internal tide is recorded during summer spring tides as brief and pulsed current surges that account for up to 40% of the total current measured near the sea floor. The currents generated by the combined action of the surface and internal tides

have created a large, isolated dune field near the shelf edge (Heathershaw et al. 1987).

On the shelf itself, the nature of the tide and tidal currents is strongly controlled by the complex 3D interaction of the tidal wave with the geometry of the shelf and shoreline. On long, straight shelves, the tide is dissipated by friction as it crosses the shelf, such that tidal currents decrease in a landward direction (Fig. 13.3). As the shelf width increases, however, it becomes closer to resonance with the semi-diurnal M2 tide: resonance happens when the tidal wave reflected by the coast is in phase with the incoming wave, which occurs where the shelf width is equal to one-quarter, or 3/4, or 5/4, etc., of the wavelength of the tidal wave, which is a function of the water depth (e.g. Pugh 1987). Due to tidal resonance, the maximum tidal range occurs when the shelf is of the order of 200–400 km wide for typical shelf depths. The influence of changing tidal range on tidal-current speed is direct, but the impact is not uniform over the entire width of the shelf; the greatest change in the strength of the currents occurs near the shelf margin because this is where the change in the tidal prism is greatest.

The situation in embayments and semi-enclosed seas is more complex, with the response of the tidal wave being dependant on the specific configuration of the sea and of its connection with the open ocean. Most open-mouthed embayments accentuate the tide because the cross-sectional area through which the tidal wave passes becomes smaller in a landward direction. Consequently, the tidal range and current speeds are generally higher in embayments than on straight shelves. Examples are given by the English Channel, the North Sea, and the Yellow Sea, and by the Gulf of Bengal, which is a tectonic embayment fully exposed to the ocean. The tidal ellipse is also more elongated and the currents tend toward being rectilinear because of the confinement by the margins of the embayment. Other types of tectonic embayments where the tide is commonly amplified include rifts and foreland basins; in fact, a significant number of the areas with tidal ranges greater than 10 m today are in such settings (Archer and Hubbard 2003). The prediction of resonance in embayments can only be done using numerical modeling, with a full knowledge of the 3D geometry of the shelf and shoreline morphology, as illustrated by studies of the funnel-shaped Gulf of Maine – Bay of Fundy system (Greenberg 1979) and the Western Channel Approaches that might have gone into and out of resonance during the early stages of the last post-glacial transgression (Uehara et al. 2006). By comparison, semi-enclosed seas such as Hudson Bay and the Baltic Sea are more likely to have small tides because the oceanic tidal wave cannot propagate into them effectively, and they are not large enough to have their own tide. Again, the specific response can only be determined by numerical modeling.

Local coastal irregularities such as headlands also perturb the tide. Horizontal flow expansion and constriction on either side of a headland brings about a complex 3D tidal asymmetry, which results in a residual flow that takes the form of time-averaged eddies on either side of the protuberance (e.g. Pingree and Maddock 1979).

Seaways and straits that connect two larger bodies of water are especially prone to pronounced accentuation of the tidal currents because of the constriction. Even a small difference in water elevation at the two ends of a strait can generate strong currents (Pratt 1990). This is the case of the Messina Strait in the modern Mediterranean Sea, despite the fact that the tidal range is less than 10 cm (Androsov et al. 2002), with dunes forming in water depths of more than several hundred meters (Colella 1990).

13.2.2 Residual Tidal Currents

Because each tidal constituent is oscillatory and symmetrical, the net flood and ebb currents should be equal and opposite. However, the examination of measured tidal ellipses show that they are not symmetrical: the peak ebb and flood currents are neither equal in speed, nor are they colinear. This is due to the distortion of the tide and/or to the interplay of more than one tidal constituent. The most important of these is the interaction of the M2 (semidiurnal) tide with its first (M4) harmonic (Pingree and Griffiths 1979; see more below).

Distortion of the tidal wave occurs due to topographic effects. As the tide moves into shallow water, it slows down because of friction, but with the trough decelerating more than the crest because the water depth is less beneath the trough. The consequence is the development of tidal asymmetry, with the front of the tidal wave (i.e., the flood tide) being steeper and of shorter duration than its back (i.e., the ebb tide). This, in turn, brings about an inequality of peak flood and ebb current speeds,

creating a tendency for the flood-tidal currents to be faster than the ebb. A similar distortion occurs if the tidal wave enters an embayment, because the progressive, offshore tidal wave cannot continue to propagate freely. Interference of M2 and M4 harmonics of the tide brings about either tidal-phase asymmetry if the M2 and M4 are 90° out of phase or tidal-current inequality if the M2 and M4 are in phase. The tidal motions will be asymmetric in either case: in the first case, the flow in one direction will last longer than in the other, and, in the second, the flow in one direction will be faster although of shorter duration.

Since bedload transport is approximately proportional to the cube of the current speed, any asymmetry in ebb and flood currents will generate inequalities in the sediment transport in the two directions. The result is the creation of a residual sediment transport in one direction (either the ebb or flood). Such inequalities extend over large areas and are referred to as tidal-transport pathways, which are discussed at length later in this chapter.

13.3 Sediment Types on Tidal Shelves

Tidal currents are fast enough on many shelves to transport sand and finer-grained sediment. Much of the existing literature concentrates on sandy deposits, but muddy tidal-shelf deposits are important in areas supplied with large quantities of mud by rivers (e.g. the Amazon and Guyana shelf, the Gulf of Bengal and the Andaman Sea, and the inner portion of the East China Sea). On these shelves, tidal currents contribute significantly to the resuspension of mud (e.g. Viana et al. 1998; Yang and Liu 2007). For example, one of the largest turbid plumes in the world occurs in the Andaman Sea as a result of tidal-current activity (Ramaswamy et al. 2004) with the resulting export of mud to deep water (Rao et al. 2005). On the Amazon shelf, the tidally resuspended mud is advected to the north by wind-driven currents and forms a near-coast nepheloid layer that reduces the bottom friction; consequently, the tide that reaches the coast is larger than would be the case otherwise (Gabioux et al. 2005; Bourret et al. 2008). In the Yellow Sea, tidal resuspension of mud from offshore deposits is responsible for the creation of sandy lags.

Most modern shelves that experience significant tidal-current action are beyond the influence of sediment supplied by rivers. Consequently, older deposits have been reworked by waves and tidal currents that have winnowed away the fine-grained material, leaving behind tidal deposits that are composed predominantly of medium to coarse sand. Such is the case around the British Isles. For the reasons discussed at length by Dalrymple (2010a), the sand becomes finer in the direction of sediment transport, such that coarser sediment, including gravel, can be present at the up-current end of tidal-transport paths, where the currents are fastest, passing down the transport path to fine and very fine sand and even muddy deposits. Tidal currents are an effective sorting agent, and the sorting index is generally high, and increases along the pathway (Gao et al. 1994).

On shelves that are not supplied by large mud-rich rivers, carbonate grains can be an important constituent of the deposits because tidal currents favor the supply and mixing of nutrients coming from the open sea, thereby promoting carbonate production. In cases where there is little or no siliciclastic material, the tidal-shelf deposits can be composed entirely of carbonate grains. In tropical settings, such tidal deposits are commonly composed of ooids, which are believed to be a type of grain formed almost exclusively in tidal settings (e.g. the Bahama Banks; see Chap. 20). In cool- to cold-water settings, herterozoan benthic communities generate abundant bioclastic debris that is particularly prone to reworking by tidal processes (cf. Anastas et al. 1997; James 1997). Tidal-transport pathways exist in carbonate environments (e.g. Harris 1988), but, in such settings, sediment grain size is more strongly controlled by the biota present than by the speed of the tidal currents.

Along a tidal-transport pathway, the nature of the substrate and the strength of the currents control the nature of the benthic biota. Areas scoured by strong currents, where the sea floor consists of exposed bedrock, are dominated by epibenthic, encrusting faunas, whereas depositional tracts with mobile sand are dominated by endobenthic faunas (Wilson 1982); in general, however, the more mobile the substrate, the less diverse the fauna will be. In the modern, relatively little study has been devoted toward linking the fauna with position along a transport pathway, although spatial variations in the composition of small bryozoan particles (Bouysse et al. 1979) or molluscan species (Reynaud et al. 1999c) have been noted. Physical and biogenic destruction of particles occurs during transport. On modern shelves,

the intensity of reworking and mixing of grains increases with water depth, as the result of increasing time and decreasing sediment supply through the post-glacial transgression (Wilson 1988). In the Miocene cool-water carbonates of SE France, recurring associations between the fauna and tidal bedforms have been noted (Descote 2010). The largest and coarsest grained dunes contain the highest content of red algae, whereas the small and finer-grained dunes show a larger amount of benthic forams and molluscans. This partitioning is also reflected in the sequence-stratigraphic organization of the deposit. The coarse bioclastic TST deposits are dominated by a bryozoa/echinoderm (Bryonoderm) fauna, which is succeeded by a red algae (Rhodalgal) association, whereas the more muddy HSTs are dominated by a mollusc/benthic foraminifera (Molechfor) association.

13.4 Tidal Dunes

The sandy sediments that are present over large parts of tidal shelves are very commonly molded into a complex array of large bedforms, ranging from flow-transverse dunes of various sizes to nearly flow-parallel tidal-current ridges. Dunes are the most ubiquitous bedforms on continental shelves, occurring both on sand ridges and flat sand sheets, and are responsible for much of the sedimentary record of offshore tidal environments. Therefore, they are discussed at length here.

13.4.1 Morphological Response to Flow

Dunes is the generally accepted term that replaces the older terms *megaripple* and *sandwave* (Ashley 1990). Flume experiments and observations in nature have defined the stability field of dunes as a function of grain size, current speed and water depth (e.g. Rubin and McCulloch 1980; Allen 1982; Southard and Boguchwal 1990). Dunes can be formed in grain sizes between approximately 0.15 mm (i.e. within the range of fine sand) and gravel size (Carling 1999), and by current speeds above about 0.5 m/s. Water depth is not a significant limiting factor on the occurrence of dunes, provided the current speed is sufficient, although an increase in water depth commonly leads to a decrease in current speed and, hence, the disappearance of dunes.

The size and shape of dunes vary widely. Following Ashley (1990) and Dalrymple and Rhodes (1995) we suggest the size distinctions given in Table 13.1. The maximum height of a shelf tidal dune is not well defined, but tidal dunes up to 15 m high are reported on modern shelves (e.g. Berné et al. 1989). The larger the dunes, the lesser their relative relief: in general, the dune wavelength-to-height ratio (= the ripple index; RI) is less than 10 for small dunes but commonly exceeds 30 for large dunes, and may reach 100 for very large ones.

The size and shape of dunes are controlled by water depth, current speed and grain size. Studying dunes in flumes and rivers, Van Rijn (1982, also Southard and Boguchwal 1990) showed that, in the lower part of the dune stability field, increasing current speed brings about an increase of the equilibrium height of dunes. As well, for a given depth and current speed, the dune height increases slightly with grain size (Flemming 1980; Van Rijn 1982). Water depth, which is a proxy for boundary-layer thickness, is generally regarded as being the most important control on dune size, with dune height (H) and wavelength (L) increasing as water depth (h) increases (Ashley 1990). Following Yalin (1964) and based on many examples in nature summarized by Allen (1982), the widely accepted relationships are:

$$L = 6h \tag{13.1}$$

$$H = 0.167h \tag{13.2}$$

These relationships are only applicable in cases where the dunes are fully developed in equilibrium with the flow, and where the sea floor is completely covered by mobile sediment, a condition called fullbedded (Ashley 1990). These relationships do

Table 13.1 Size classes for dunes (From Dalrymple and Rhodes 1995)

	Small	Medium	Large	Very large
Wavelength (L)	0.6–5 m	5–10 m	10–100 m	>100 m
Height (H[a])	0.05–0.25 m	0.25–0.5 m	0.5–3 m	>3 m

[a] Calculated from the Flemming (1988) relationship: $H = 0.0677\ L^{0.8098}$

not apply in deep water where the thickness of the boundary layer, the real control on dune size, is less than the water depth, or to the smaller dunes that are superimposed on the larger dunes in an area to form compound dunes (Ashley 1990). The size of these smaller dunes is generally thought to be related to the presence of an internal boundary layer that is formed on the back of each larger dune (Rubin and McCulloch 1980; Dalrymple 1984).

Because of the widespread occurrence of unidirectional residual sediment transport in tidal-transport pathways, the dunes on tidal shelves are typically strongly asymmetric, with their steeper, lee face inclined in the direction of net sediment movement. In tidal settings, weakly asymmetric dunes, although not common, can be found in areas of weak tidal asymmetry. The speed of dune migration in the direction of residual transport increases as their asymmetry increases, but decreases as their size increases, all else being equal. The average annual distance of migration of small dunes is about 100–300 m, while it is only 25–75 m for large ones and only a few decimeters for very large dunes (e.g. Fenster et al. 1990). The *lag time* of the dunes (i.e. the time needed for them to equilibrate with a changed flow condition) also increases as they become larger; thus, large and very large dunes on the seafloor have the potential to be out of equilibrium with the present-day flow. Also, as the dunes become larger and less active, they have the potential to become more bioturbated.

Although dunes are most commonly oriented with their crest nearly perpendicular to the flow, tidal dunes can be oblique to the peak tidal flow and to the residual transport of sand. Theoretically, this occurs where dominant and subordinate tidal currents are not colinear, with the degree of obliquity depending on the ratio of sediment transport by the dominant and subordinate currents (Rubin and Hunter 1987; Rubin and Ikeda 1990). In shelf settings, however, the dominant and subordinate currents are typically nearly 180° apart, but, despite this, the dunes can be oblique, with the amount of obliquity typically increasing as the dunes become larger. The most widely held suggestion as to why this occurs is that large dunes reflect the impact of infrequent events such as intense storms and wind-driven currents that have higher sediment-transport capacity than the more frequent, but weaker, tidal currents. Also, the obliqueness of large dunes could reflect flow-transverse variations in their migration rate, as a result of inequalities in sediment discharge and bedform height (Dalrymple and Rhodes 1995). Although the smaller dunes may have more variable orientations over large areas, they statistically provide a more reliable indication of the *local* peak tidal-current direction than the large dunes.

13.4.2 Internal Structure of Offshore Tidal Dunes

The available knowledge on the internal structure of tidal dunes comes mainly from studies in modern estuarine settings (Dalrymple 1984), with additional observations from ancient shallow-water successions (Allen and Homewood 1984). Very few observations of the internal structure of shelf dunes exist, and most of those come from seismic records (e.g. Berné et al. 1988, 1989), which do not have sufficient resolution to show the detail seen in outcrops.

The internal structure of simple dunes (i.e. dunes that lack superimposed dunes; Ashley 1990), regardless of size, consists of foreset laminae emplaced by pulses of grain flow on the lee face, which is inclined at an angle close to the angle of repose (ca. 32–35°), and toeset and bottomset laminae that accumulate by the settling of grains from suspension. This produces crossbeds that can extend over hundreds of meters laterally (Fig. 13.4) if formed by a large to very large dune; smaller dunes produce crossbeds of lesser lateral extent. As it is steep, the lee face of a simple dune promotes flow separation and, therefore, possible up-dip migration of ripples on the toesets (Fig. 13.5a). The tidal-bundle successions produced by neap-spring tidal cycles can be present in offshore dunes (e.g. Longhitano and Nemec 2005), but are not likely to be developed extensively because dunes on shelves are typically too large, and move too slowly, to record variations in flow speed and direction over individual tidal cycles. Thus, grain-size segregation in the foreset lamination, which is sometimes referred to as *grain striping*, is generally not related to changes in the speed of the tidal currents, but rather to the effect of pre-sorting of sediment by small superimposed bedforms (Reesink and Bridge 2007, 2009). Similarly, convex-up erosion (reactivation) surfaces within the upper part of these crossbeds (Fig. 13.5a), which are classically attributed to erosion by the subordinate tide (Allen 1980), are more likely to

Fig. 13.4 Succession of vertically stacked carbonate crossbeds formed by simple, large to very large dunes migrating under the influence of unidirectional or highly asymmetric tidal currents, Bonifacio Formation, Corsica (see Brandano et al. 2009; André et al. 2011). The exposure shown is about 25 m high. The vertical stacking of such thick crossbeds in successions up to hundreds of meters thick (250 m in the Bonifacio Formation) is a characteristic feature of the infill of tidal seaways or straits where accommodation is high. The prominent crossbed boundaries correspond to intervals deeply bioturbated by *Thalassinoides*

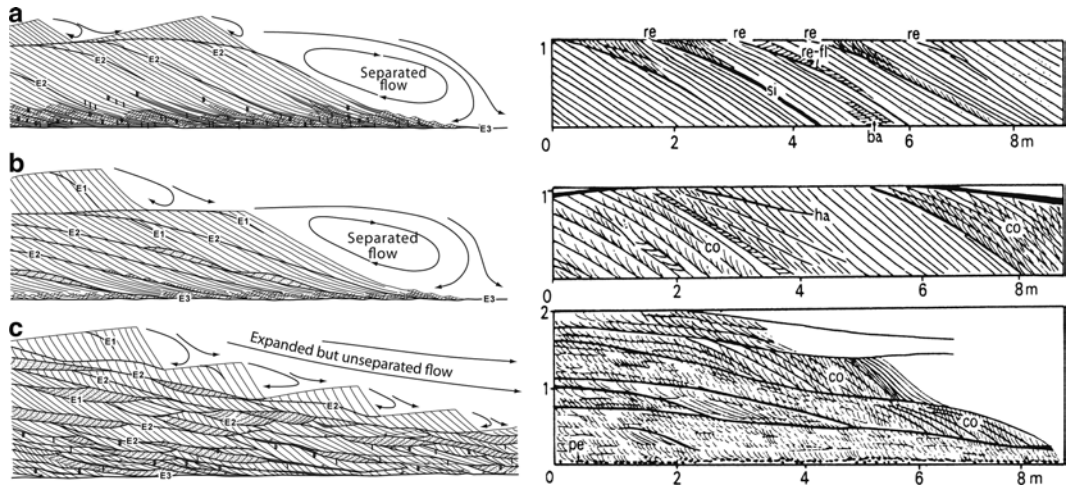

Fig. 13.5 (*Left*) Internal structures formed by compound dunes. Slopes of foresets range from 35° (laminae) to 4° (master beds in **c**). The internal complexity depends on the relative size of the 'master' and superimposed dunes, which controls the amount of erosion on the lee of the large dune and therefore its overall steepness (After Dalrymple 2010b), modified in part from Allen 1980). (*Right*) Outcrop sketches of compound-dune deposits in the Precambrian Lower Sandfjord Formation, Norway (After Levell 1980). *Re* reactivation surfaces, *si* silt drapes, *re-fl* reverse-flow ripples, *ha* hanging set boundaries, *co* convex-up boundaries, *pe*: pebble horizons

be generated by erosion in the troughs of superimposed dunes as they migrate over the brink of the larger bedform (Dalrymple 1984, 2010b; Reesink and Bridge 2009), or to episodic wave action. It is important to note that mud drapes, which are an important signature of tidal sedimentation in estuarine and deltaic settings (Visser 1980; Nio and Yang 1991; Dalrymple 2010b), are rare in offshore tidal deposits because of the presence

of rotary tides with no distinct slack-water period, and because suspended-sediment concentrations are generally very low.

Large and very large dunes are typically covered by smaller dunes and have a compound morphology. Such dunes generate *compound crossbedding*, composed of stacked, inclined, planar to trough crossbeds formed by the superimposed smaller dunes (Fig. 13.5b, c). The lee side of compound dunes typically has a much lower slope (commonly <10°) than that of simple dunes. Flow separation does not occur, and the smaller, superimposed dunes migrate continuously down the larger dune's lee side, from the crest to the trough. Flow expansion and flow deceleration bring about deposition on the lee side of the larger dune, so that each superimposed smaller dune leaves behind a crossbed that gets preserved. The continuous accretion of such crossbeds forms the master bedding of the compound dune. The superimposed dunes may themselves be compound, so that 'compound-compound' dunes can occur (Anastas et al. 1997). It is noteworthy that the smaller dunes migrate in essentially the same direction as the larger dune, forming an architecture termed *foreward accretion*. Upslope-climbing ripples or smaller dunes formed by the subordinate current are likely to be preserved, forming herringbone cross-stratification. Tidal-current reversals are generally not capable of generating master-bedding surfaces in large to very large dunes, because the time required for such large dunes to reverse greatly exceeds the duration of a tidal cycle. For example, the time needed for a 4 m-high dune to reverse is about 200 days of continuous bedload transport, based on an average rate of transport typical of tidal environments (Dalrymple and Rhodes 1995). Longer-term flow reversals, such as those associated with seasonal changes in the wind regime or ocean circulation, could, however, cause dune reversal and the creation of master-bedding planes. Similarly, high-energy storms with greatly increased sediment-transport rates could also bring about dune reversal (Houthuys et al. 1994; Le Bot and Trentesaux 2004). The storm-wave activity can also erode the crest of the dune, generating horizontal erosion surfaces (e.g. McCave 1971; Dalrymple 1984; Berné et al. 1991).

The vertical succession of structures produced by a compound dune generally coarsens upward, and the individual cross beds in it commonly become thicker upward (Fig. 13.5). The upward-coarsening trend is caused by the fact that the shear stress exerted by the flow is higher at the crest than in the trough of the compound dune. The downward thinning occurs due to the fact that the superimposed dunes become smaller as they migrate down the larger lee face because they are losing sediment to the cross bed that they leave behind (Rubin 1987). The bottomset region of compound dunes is the area where muddy deposits are more likely to occur; bioturbation is also greater there than elsewhere.

13.5 Offshore Tidal Ridges

Tidal-current ridges are widely developed on tidal shelves and comprise a significant fraction of the total volume of all sandy deposits in the modern. They are the largest bedforms that exist, reaching 200 km in length, 10 km in width and 50 m in height. Offshore tidal ridges generally occur as fields of regularly spaced, parallel *en echelon* ridges (Off 1963) that can cover tens of thousands of square kilometers, as in the Celtic Sea, the North Sea, and the East China and Yellow seas (Fig. 13.6). They may also occur as isolated ridges in the lee of islands and capes (in this case they are called *banner banks*). Offshore tidal ridges are made up by the accretion, at the largest scale, of the crossbeds formed by dunes.

13.5.1 Ridge Morphodynamics

Unlike dunes, ridges are not the expression of the turbulence of the primary flow at the seabed and the related local advection of sediment. The ridges occur in rotary 'cells' within tidal-transport paths where the residual transport retains a higher proportion of the sediment that is in transit. Within these cells, ridges grow in place of flat sand sheets: sediment moves in opposite directions on either side of the ridge crest, with the potential for sand to circulate around bank terminations (McCave and Langhorne 1982; Howarth and Huthnance 1984). Near the coast, these cells can correspond to the eddies that are generated by a headland (Fig. 13.7; Pingree and Maddock 1979). Further from the shore, on the open shelf where linear ridges develop, the rotary circulation is the result of a positive feedback between the reversing tidal flow and the topography of the ridge (Zimmerman 1978; Pan et al. 2007). This rotary residual transport of sand is driven

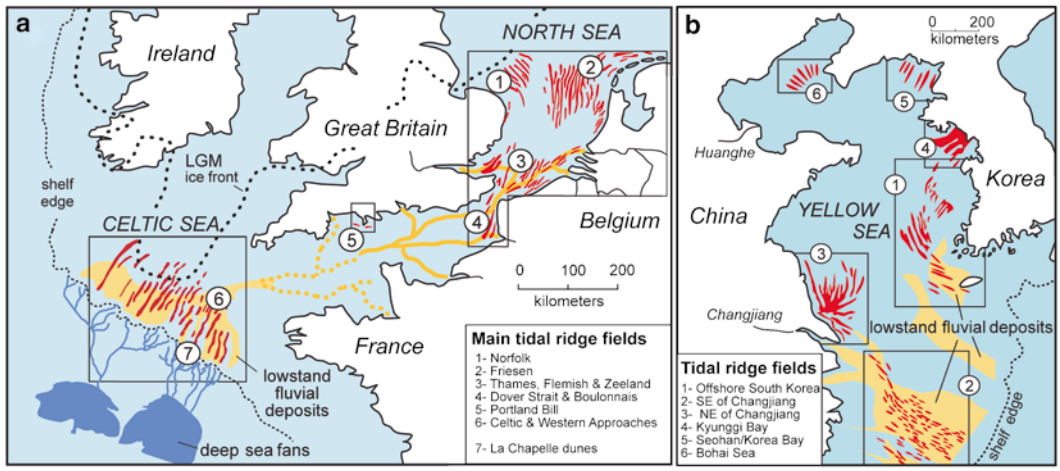

Fig. 13.6 Map showing the distribution of the major tidal ridges (**a**) on the Western European shelves and (**b**) the East China and Yellow seas. All the ridges are linear, offshore 'en echelon' tidal ridges, except those in location 5, which are banner banks associated with a headland. In (**a**), ridge field 1 occurs on a headland-associated shoal-retreat massif (Swift 1975). Ridge field 2 might also occupy a shoal-retreat massif; alternatively, it may represent the redistribution of an east-west-oriented barrier complex that existed earlier in the post-glacial transgression. Ridge fields 3 and 4 may represent an embayment-head type of occurrence (cf. Dyer and Huntley 1999). In (**b**), note the train of tidal ridges along the retreat path of the Changjiang River (ridge field 2). Ridge field 1 may occupy the retreat path of the Huanghe and/or Han River

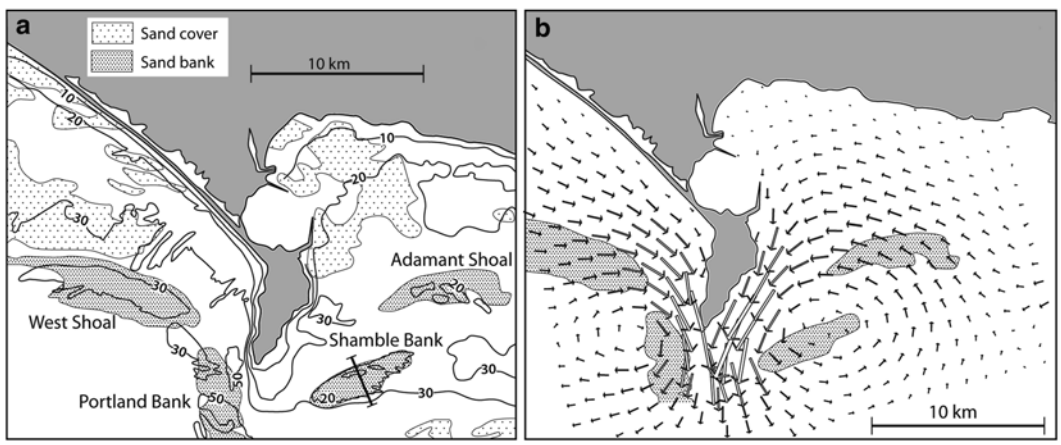

Fig. 13.7 (**a**) Tidal ridges around the Portland Bill headland, English Channel (see location in Fig. 13.6a – ridge field 5). These are typical 'banner banks' that form in the lee of coastal promontories (After Bastos et al. (2003). (**b**) Numerical model of tidal residual circulation (After Pingree and Maddock 1979). Bedform migration directions on Shamble Bank are consistent with the counterclockwise circulation of the modeled eddy. The observed convergence of bedload transport toward the centre of the eddies is explained by a centripetal reduction of bottom shear stress (see detailed explanation in Dyer and Huntley 1999). The process is efficient for small eddies only (ca. 10–20 km in diameter), implying that this process cannot generate longer ridges

by two vorticity forces that increase toward the ridge crest, one due to the increase of bottom friction in the shallower water over the crest, and the other due to an enhanced Coriolis effect (Fig. 13.8). The Coriolis effect either dampens or enhances the friction-driven circulation, depending on whether the ridge is oriented clockwise or counter-clockwise, respectively, to the peak tidal flow. This explains why ridges are mostly skewed in a counter-clockwise sense relative to the peak tidal flow in the northern hemisphere (Fig. 13.9).

The growth of a linear shelf ridge from a small bed perturbation (bump) was first modeled by

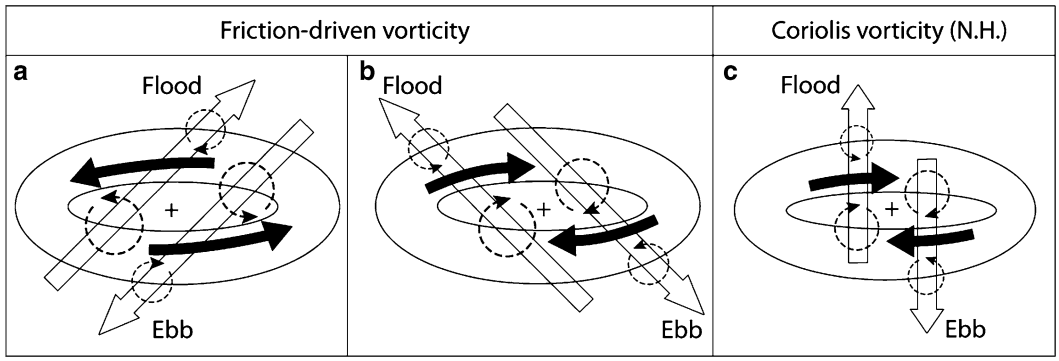

Fig. 13.8 (**a**, **b**) Friction-driven vorticity (*dotted circles*) induced by oblique flow across an elongated bump on the seabed. The open *straight arrows* show the flood and ebb current vectors. The *black arrows* show the resulting residual circulation around the bump (i.e. the tidal ridge). The vorticity increases toward the top of the ridge, acting to move bedload toward the ridge crest. (**c**) Coriolis-driven vorticity induced in the northern hemisphere (*N.H.*) by the flow across the same seabed relief. This results in a clockwise residual circulation (counter-clockwise in the southern hemisphere). This effect enhances or damps the friction-driven residual circulation. In the northern hemisphere, their interplay favors the existence of ridges oriented counter-clockwise to the flow (After Pattiaratchi and Collins 1987)

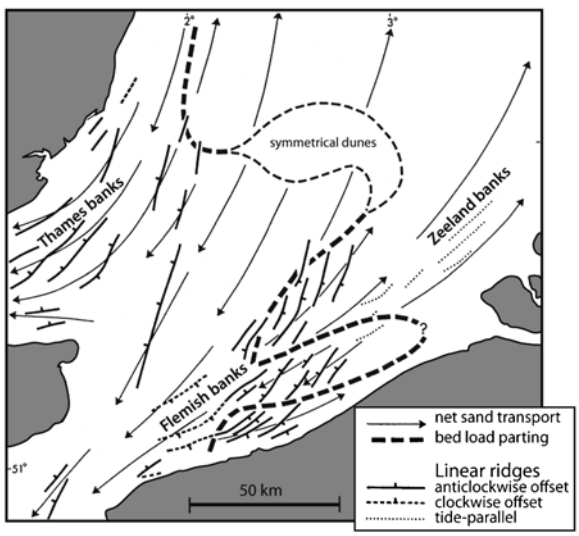

Fig. 13.9 Tidal ridges and tidal-transport pathways in the southern North Sea (ridge field 3 in Fig. 13.6a). Note the alignment of the ridges at a small angle to the net sand-transport paths, which have been determined from the asymmetry of dunes. Most ridges are offset counter-clockwise to the tidal flow, in response to the mechanism described in Fig. 13.8 (After Kenyon et al. 1981)

Huthnance (1973, 1982a, b). The main process involved in the Huthnance model is that the bottom friction associated with the bump delays the upslope current more than it accelerates the downslope one. As a consequence, the transport of sand toward the ridge crest will be higher than the off-ridge transport, thereby causing ridge growth. The transport paths over the ridge reflect the convergence of sediment toward the ridge crest, as noted first by Van Veen (1936). On the side of the ridge facing it, the dominant current is accelerated by flow constriction and the subordinate current is decelerated by flow expansion, so that the residual transport by the regionally dominant current is enhanced (Fig. 13.10). On the ridge side facing the subordinate current, the dominant current is weaker because of sheltering and the subordinate current is accelerated toward the ridge crest by flow constriction, so that the residual transport on this side is commonly dominated by the regionally subordinate current.

Huthnance (1982a, b) calculated that the ridges must become elongated and oblique to the peak flow at an angle of about 20°. Ridge elongation is proportional to the elongation of the tidal ellipse, and the initial bump from which a ridge grows does not have to be elongated or properly oriented itself. Based on tidal ridges in the China and Yellow Seas, Liu et al. (1998) suggest that linear ridges are restricted to areas where tidal M2 ellipticity (i.e., the ratio between the minor and major axes of the tidal ellipse) is < 0.4 (i.e., the tidal ellipses are significantly elongated), whereas sand sheets occur where the currents are more rotary. Hulscher (1996) showed that linear ridges are more prone to develop in deeper water, because the 3D flow structure is more homogenous and there is, therefore, a smaller phase lag between shear stress and the depth-averaged current speed. Theory indicates that ridges

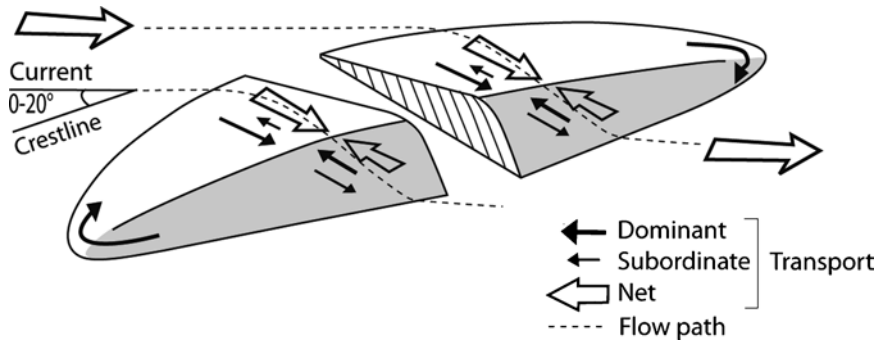

Fig. 13.10 Conceptual model of flow over an offshore tidal ridge that is slightly oblique to the tidal currents. The bending of the flow across the ridge is a consequence of friction at the seabed, which delays the shallower edge of the flow. The crest of the ridge is a convergence zone because of opposed net transport directions on either side of the ridge crest. The circulation of sand around the ends of the ridge has been documented by McCave and Langhorne (1982) and Howarth and Huthance (1984), but it is not a requirement for ridge formation (After Houbolt 1968 and Caston 1981)

must have a spacing that is of the order of 250 times the water depth (i.e. ridge spacing is many kilometers) in order for the residual rotary circulation to be established (Huthnance 1982a). This prediction is supported by observations and may explain why linear tidal ridges are largely restricted to open shelves and seem to be absent in narrow seaways (Harris 1988; Malikides et al. 1988).

13.5.2 Ridge Architecture

As a consequence of the tidal asymmetry, the ridges migrate in the direction of the dominant regional current, but at a rate that is so slow that it cannot be measured with confidence over a few years (Lanckneus et al. 1994). Because of the slight obliqueness of the tidal flow relative to the ridge axis, the ridges migrate laterally, as documented first by Houbolt (1968) (Fig. 13.11), especially in areas with a strong residual transport. In areas of weaker tidal asymmetry, accretion can occur on both sides of the ridge (Davis and Balson 1992). Banner banks, because they are anchored in a coastal eddy, may be aggradational rather than migratory (Fig. 13.11). Lateral migration and aggradation are likely to be disrupted during periods of increased storminess, which can either accelerate deposition or cause significant erosion of the crest, producing flat, wave-planation surfaces, as showed for Sark and Shamble banks in the Western Channel (M'Hammdi et al. 1992; Bastos et al. 2003; Fig. 13.11). Although accretion on the regional down-current flank might be most common, accretion can occur on the side facing the dominant current (McCave and Langhorne 1982; Dalrymple and Rhodes 1995; Reynaud et al. 1999b; Fig. 13.12). This happens when the ridge height is a significant fraction of the water depth, such that bottom friction, which slows the flow toward the ridge crest, is greater than the tendency for acceleration as a result of the flow constriction. In this case, the cross-ridge flow can become accelerated through local low points along the crest, forming oblique channels called *swatchways*. These channels can then lead to splitting of the ridge into two, *en echelon* parts as described by Caston (1972) (Fig. 13.13). By this mechanism, the ridge field can expand throughout the area of the tidal transport pathway, provided there is sufficient sand.

It must be stressed that the available knowledge on the internal structures of offshore tidal ridges is based almost entirely on seismic data and surface morphology. Therefore, it is difficult to propose a generalized facies model that can be used to interpret the rock record. From the facies point of view, it is likely that the deposits within tidal ridges are composed predominantly of crossbedded sand produced by the dunes that mantle the ridges in most situations. However, it is also likely that the deposits record, at least locally, the imprint of storm waves, in the form of gravel lags with large gravel wave ripples, coarse graded storm beds or even HCS if the grain size is too fine to form dunes (cf. Yoshida et al. 2007). Because of the very large sediment volume within a ridge, one or more storms will not destroy the ridge but can be very prominently recorded in its architecture and facies (Houthuys and Gullentops 1988a, b). The deposits are thought to

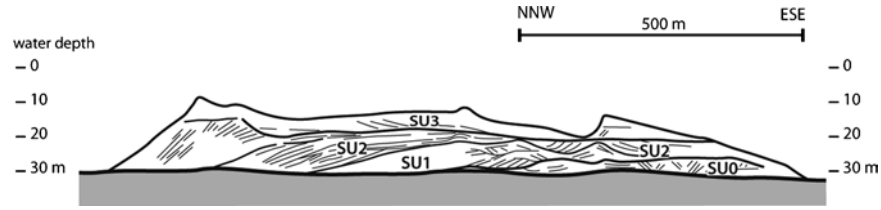

Fig. 13.11 Transverse cross-section of Shambles Bank in the English Channel (see also Fig. 13.7). The flat erosional surfaces that constitute the main master bedding may be the result of erosion by storm waves. The pattern is partly aggradational, because the sand is trapped in the residual eddy that determines the location of the bank. The large superimposed dunes produce compound crossbeds with cosets over 6 m in thickness (After Bastos et al. 2003)

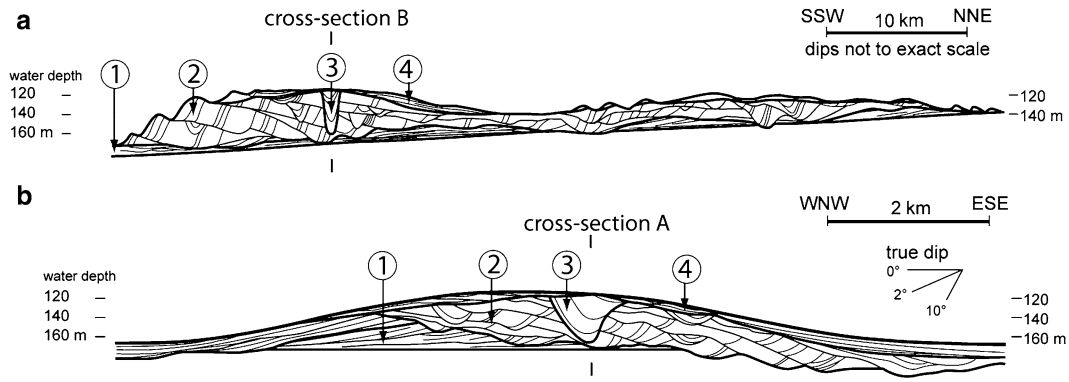

Fig. 13.12 Longitudinal and transverse sections through a deep-shelf tidal ridge in the Celtic Sea. The units are: *1* flank deposits of the early stage of ridge growth; *2* climbing, very large compound dunes of the high-energy phase of ridge growth; *3* swatchway channel cut through the ridge by strong, cross-ridge tidal flows when the ridge crest was shallowest; and *4* abandonment deposits formed by destructive reworking of the ridge crest by wave action after active growth ceased. Dominant current was to the SW. See Fig. 13.6a (area 6) for location (After Reynaud et al. 1999b)

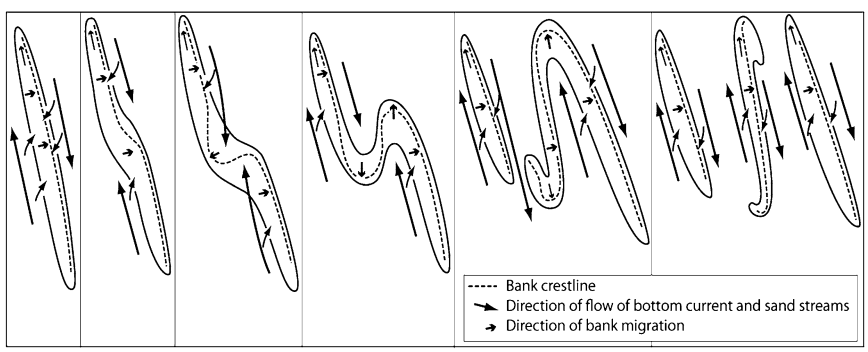

Fig. 13.13 Sequential model of ridge evolution and splitting, based on the Norfolk Ridges (see location in Fig. 13.6a, ridge-field 1). The process of ridge splitting is probably initiated by the development of a cross-ridge swatchway (in steps 2 and 3 from the *left*), which grows in size until the original ridge separates into two parts (After Caston 1972)

coarsen upward, because current speeds and wave action are highest on the ridge crest. If, however, the ridge becomes large enough that it impedes cross-ridge flow, then there may be a tendency for finer sediment to accumulate in the area of weaker currents on the ridge crest. As we will see later, however, the sea-level history during ridge growth and migration can be significant, because ridges are so large that their lag time is likely to be of the same order as the duration of a high-frequency sea-level cycle.

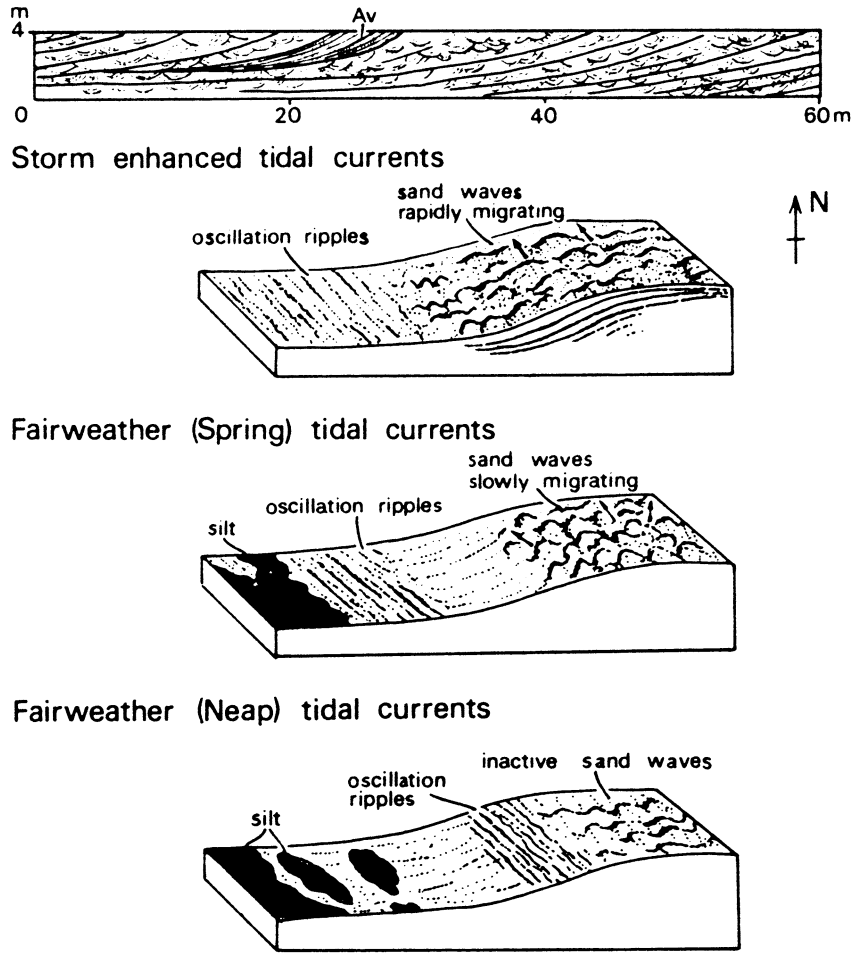

Fig. 13.14 Depositional model for a tidal shelf ridge, based on the Precambrian of north Norway. The ridge is interpreted to be shore-parallel and separated from the coastline by an area of wave erosion. The upper part of the ridge is composed of cross-bedded sandstone created by the along-strike migration of dunes ('sand waves'). Channels cut by bidirectional currents dissect the ridge crest. The ridge growth and migration is related to storm-enhanced tidal activity. It passes gradually offshore to muddy, storm-influenced facies (From Johnson 1977)

13.5.3 Ridges in the Rock Record

There are very few detailed case studies in the ancient that argue convincingly for the existence of tidal-current ridges. The Mutti et al. (1985) model for a 'tidal bar' shows an upward-coarsening succession and the presence of dune cross bedding as predicted from modern tidal ridges, but it shows forward accretion instead of the lateral accretion documented from modern examples. Therefore, the bedforms described by Mutti et al. (1985) are more likely to represent very large compound dunes (cf. Fig. 13.4; Dalrymple 2010b). The Johnson (1977) model for tidal ridges (Fig. 13.14) is more consistent with modern examples because of the presence of lateral accretion and upward coarsening, but the suggestion that migration is always in an offshore direction is inconsistent with many modern examples. The absence of a basal erosion surface is also not what is seen in modern shelf ridges. Erosionally based shelf sand bodies have been documented from the Cretaceous Western Interior Seaway of Northern America (Tillman and Martinsen 1984), but they have been reinterpreted as forced-regressive shorefaces and deltas, detached from the coast by subsequent transgressive ravinement (Walker and Bergman 1993; see Chap. 17).

13.6 Tidal-Transport Pathways

13.6.1 General Characteristics

As has been discussed already, the asymmetry of the tidal currents that results from the complex interaction of the tidal wave with the shelf and shoreline morphology, or with other currents (e.g., storm, wind-induced or geostrophic currents; Flemming 1980; Suter 2006), leads to the existence of *tidal-transport pathways* that extend over large areas. In each pathway, there is unidirectional residual transport of sediment that is reflected in the grain-size of the sediment and the spatial distribution and facing direction of bedforms (e.g. Grochowski et al. 1993; Fig. 13.15). In areas surrounding the British Isles where they are documented in detail, such tidal-transport pathways stretch for tens to hundreds of kilometers (Fig. 13.16). Sand is transported away from erosional areas referred to as *bedload partings* (i.e. locations where the directions of residual transport diverge; Harris et al. 1995), and moves along the transport pathway, much of which is a bypass zone (Stride 1963; Kenyon and Stride 1970; see summary in Johnson et al. 1982). In general, current speed decreases along the length of a transport pathway. Consequently, the sand becomes finer in the residual down-current direction, and is deposited as the transport capacity decreases. The location of the site of maximum deposition, and hence the thickest deposits, depends on the rate of decrease of transport capacity and does not need to be located at the end of the transport pathway. The maximum net deposition might also occur where two pathways meet (i.e. a *bedload convergence* zone), as it is the case to the west of the Strait of Dover (Fig. 13.15).

Smaller scale tidal-transport pathway can also be created by topographic constrictions. For example, straits can create localized areas of scour because of flow acceleration through the narrows. On the other hand, the flow exiting from the constriction experiences flow expansion leading to sediment deposition. Because of the reversing flow, deposition can occur at both ends of the strait, which acts as a localized bedload parting. Several examples of such accumulations have been documented from the rock record. The deposits associated with the straits can take the form of extensive sand sheets (with or without tidal ridges) or more localized delta-like bodies (e.g. Kamp et al. 1988; Reynaud et al. 2006; Fig. 13.17). Because these topographically controlled tidal-transport pathways are spatially more restricted than those occurring on open shelves, crossbedded sands can pass laterally to finer-grained, non-tidal facies over only a few kilometers (Bassant et al. 2005).

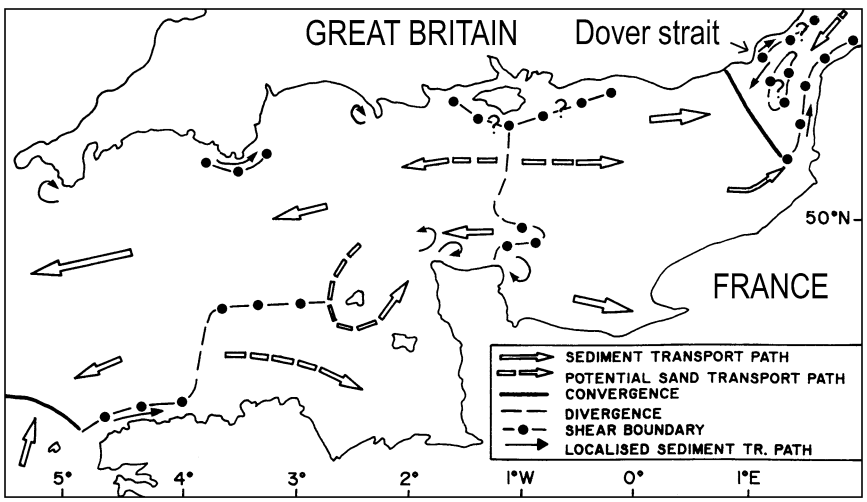

Fig. 13.15 Residual bedload transport directions in the English Channel, based on hydrodynamic modeling of tidal currents. The modeled tidal-transport pathways is in good agreement with the transport directions deduced from active bedforms, except in the Strait of Dover where the convergence zone lies further to the north (After Grochowski et al. 1993)

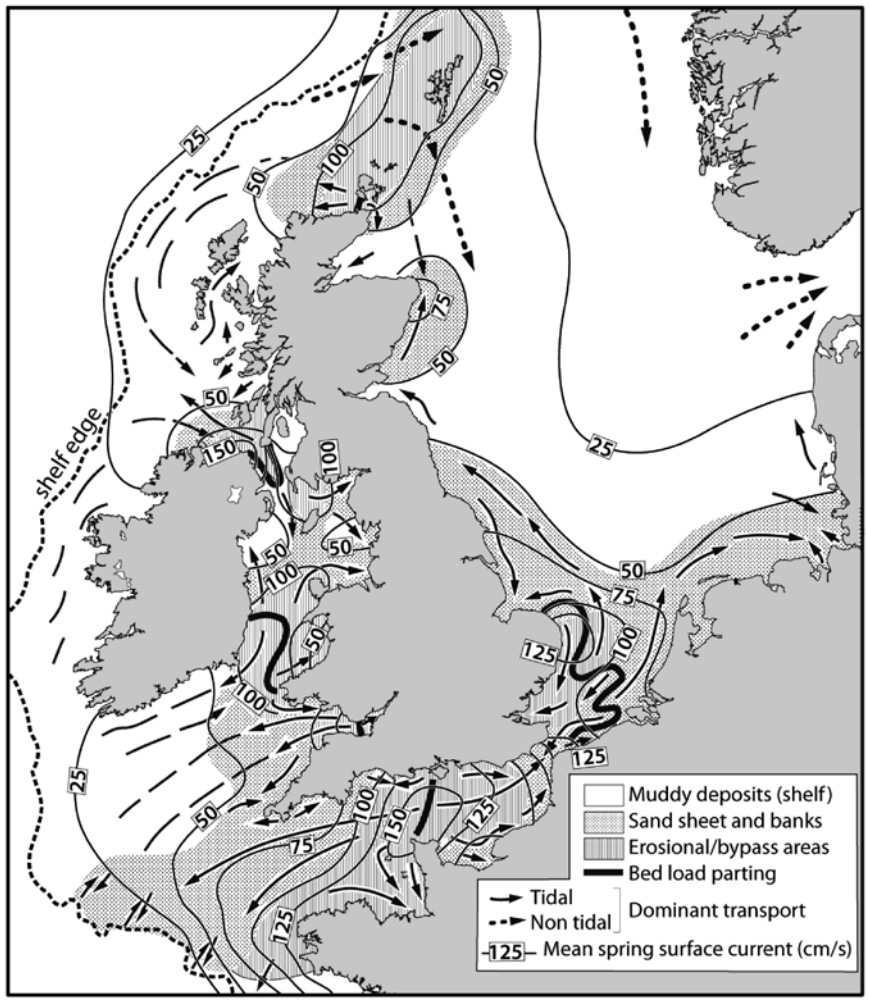

Fig. 13.16 Sea-floor sediment type, surface currents and tidal-transport pathways around the British Isles. Arrows show potential bedload-transport directions that diverge from erosional bedload partings, to convergence areas where deposition occurs (After Howarth 1982 and Johnson et al. 1982)

13.6.2 Bedform Distribution

A predictable progression of bed features occurs along a tidal-transport pathway as a result of changes in the sediment regime (Belderson et al. 1982; Fig. 13.18). In erosional, bedload-parting areas, older deposits are exposed or are covered by a patchy veneer of lag gravel and sand. Erosional features include current-parallel furrows and flute-shaped depressions. Mobile sand in these areas occurs as sand shadows in the lee of bedrock obstacles and as current-parallel sand ribbons. Subaqueous dunes can be present on the sand ribbons. As sand begins to become more abundant down the transport pathway, fields of dunes that migrate in the direction of the residual transport begin to form. In regions of limited sand, the dunes are separated by areas with no sand cover (i.e., they are 'starved') and have a barkhanoïd shape (Fig. 13.18b). If there is a larger amount of sand, the dunes coalesce to produce tidal sand sheets (Fig. 13.18a) and, under proper conditions, tidal sand ridges (Fig. 13.18c). At the extreme end of the transport pathway, sheets and patches of rippled fine and very fine sand occur where the current speed is below the critical velocity for dune stability.

As discussed above, the upper limit on dune size is controlled by the thickness of the boundary layer, which is approximated by water depth in many situations. However, current speed, grain size and sediment

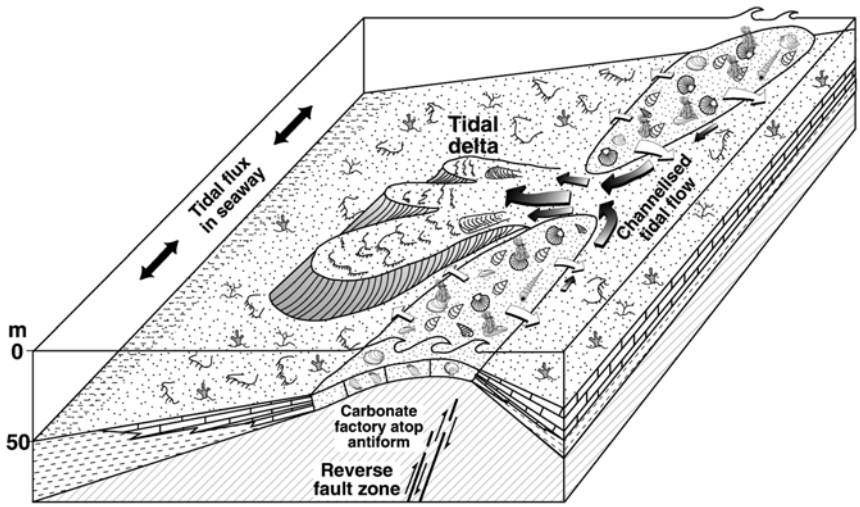

Fig. 13.17 Subaqueous, delta-like body formed of bioclastic carbonates at the 'mouth' of a subaqueous channel that cut through the low part of an anticlinal ridge in the Pliocene forearc basin of the Northern Island of New Zealand. The delta deposits consist in giant tabular crossbeds, with sets 10–40 m thick and foreset dips of 7–36°. The delta pinches out basinward into fine-grained deposits (From Nelson et al. 2003)

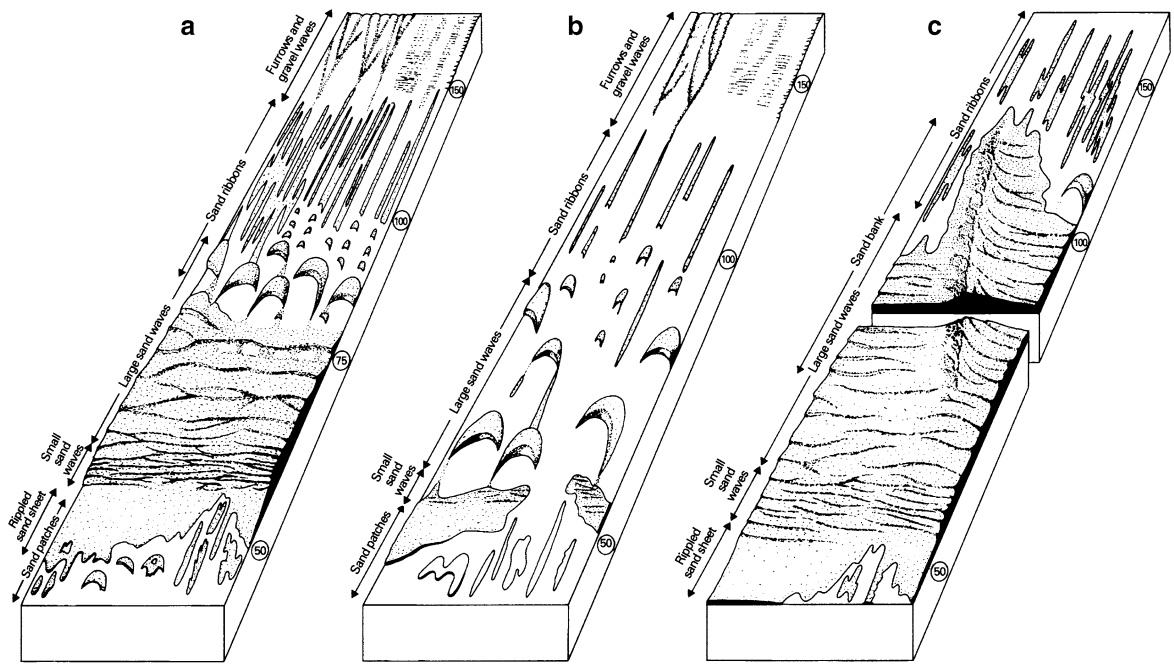

Fig. 13.18 Schematic diagrams showing the spatial distribution of bedform types along tidal-transport pathways (net sediment transport is toward the front of the diagram): (**a**) intermediate case; (**b**) regions with limited sand; and (**c**) areas with abundant sand. The up-current area in all examples experiences net erosion, whereas the downstream portion experiences net deposition because of the down-current decrease in current speed (numbers in circles). In (**c**), tidal sand ridges (tidal sand banks) occur in the upcurrent (higher current speed) portion of the depositional area. Such ridges pass down-current into a tidal sand sheet that is mantled by dunes. All of the features shown are part of the 'transgressive lag' that mantles a flooding surface (From Belderson et al. 1982)

availability also influence the size to which dunes grow. At the scale of an entire tidal-transport pathway, the dunes decrease in size along the pathway due to a decrease in tidal-current speed and grain size (Fig. 13.18a). Thus, the largest dunes are commonly found a short distance down-flow from the point where significant deposition occurs within the pathway, because this is where the current speed, grain size and sediment availability are greatest. At a smaller scale, the dunes in sand sheets are commonly grouped in isolated dune fields that are surrounded by an immobile substrate (e.g. Reynaud et al. 1999a). By contrast to what happens at the larger scale, the dunes in a dune field commonly increase in size in the down-flow direction, because of the increasing amount of available sand. As the dunes get bigger, they also get less mobile, with the larger ones tending to trap sediment brought to them by more rapidly migrating smaller dunes. Sand may not be able to escape from them; consequently, the dune field can terminate abruptly with the largest dunes near or at their leading edge. Within sand-ridge fields, scour in the troughs between the ridges commonly exposes older deposits that can be an internal source of sediment. The coarse-grained, shelly lags that occur in the troughs correlate to, and may be laterally continuous with, the lag facies in the bedload-parting area.

13.6.3 Deposits

Evidence of the former existence of tidal-transport pathways is likely to be preserved on flooding surfaces in ancient successions that contain evidence of tidal action. Over large areas, this evidence will consist of a marine erosion or 'ravinement' surface (see more below) that is mantled by a thin lag. In a down-transport direction, the deposits on this surface will thicken, potentially reaching a few tens of meters in thickness. The most volumetrically significant facies will consist of cross-bedded sands formed by dunes that were part of isolated dune fields, or of more extensive sand sheets and tidal-current ridges. The deposits of tidal-current ridges have been discussed above; here, we examine the deposits of sand sheets (Fig. 13.18a).

Little is known about the organization of these deposits, but we hypothesize that the vertical succession produced by a sand sheet consists of a stacked succession of simple and compound-dune deposits (Fig. 13.5), produced during an episode of increased tidal activity and areal expansion of the bedload parting area because of the transfer of sand to the depositional area (Harris et al. 1995). The lower part of this succession should coarsen upward, with an upward increase in the scale of the crossbeds, as a result of a 'progradation' of up-flow parts of the sand sheet over its more distal portion (Fig. 13.19a). As progressively larger bedforms migrate into the area, the scour surfaces at their base might become more prominent, potentially removing significant a amount of the pre-existing succession. If migration of the sand sheet continues, the succession will be overlain by an erosional surface corresponding to the bypass zone at the upcurrent-end of the transport path (Fig. 13.19a). If, instead, flow speeds decrease because of a change in the tidal regime, then the dunes on the sand sheet should become smaller and finer grained, generating an overall upward fining succession at the top of the sand-sheet deposit.

Full development of such a succession, with a lower upward coarsening/thickening part and an upper upward fining thinning of crossbeds, requires a relatively abundant supply of sediment. Mellere and Steel (1996) and Blackwood et al. (2004) describe successions from a seaway setting that show strong similarities to this model. Perhaps the closest match has been described from a cool-water carbonate environment (Anastas et al. 2006; Fig. 13.19b). In this case, the succession has been interpreted to reflect the migration of an area where the tidal current is above the threshold of dune formation rather than a change of current speed as a result of sea-level rise, but the result of these two processes may be difficult to distinguish. At the fringe of that area, patch reefs are present and there is a tendency for the development of hardgrounds (cf. Fig. 13.19b).

Strong tidal currents are commonly correlated with the supply of nutrients, so that the deposits in tidal sand sheets are likely to be bioturbated and, even in siliciclastic settings, to contain shelly fauna (Wilson 1982). If the dunes in a tidal-transport pathway migrate rapidly, then the intensity of bioturbation will be low, whereas dunes that migrate slowly (i.e. the larger ones, or those toward the distal end of a tidal-transport pathway) can be bioturbated more thoroughly. In general, the bottomsets of the dunes will be more intensely bioturbated than the foresets. The assemblage will be a mixed *Skolithos-Cruziana* Ichnofacies (Seilacher 1967; Ekdale et al. 1984; MacEachern et al. 2005), with vertical burrows subtending from the erosion surfaces that

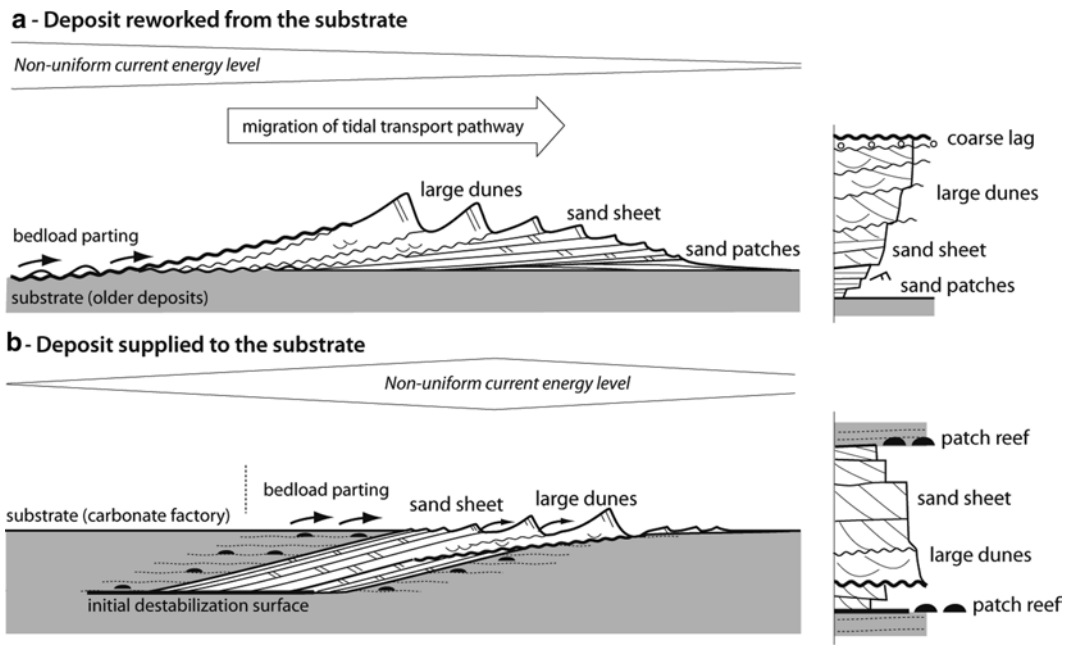

Fig. 13.19 Space-thickness diagrams showing the successions created by a tidal-transport pathway in (**a**) a siliciclastic setting where most sediments are reworked from older deposits and (**b**) a carbonate environment with significant *in situ* production. Note the difference with regard to where the deposit occurs relative to the area of strongest currents. Progressive sediment starvation in the siliciclastic setting and down-flow migration of facies zones take place as the zone of seafloor erosion expands (cf. Harris et al. 1995), producing an upward-coarsening succession topped by an erosional lag. The carbonate system, by contrast, is not sediment starved and records a more symmectrical upward-coarsening/upward-fining succession that forms as a result of migration of the dune field over lower-energy deposits, followed by gradual abandonment as tidal-current speeds decreases while transgression proceeds. Patch reefs are inferred to occur in proximity to the dune field in the carbonate example, because nutrients are supplied by the tidal currents. Cross sections not to scale, but sediment thicknesses can reach 30–50 m in both situations. The horizontal extent is tens of kilometers. (Sketches based on Belderson et al. 1982 and Anastas et al. 2006, respectively)

separate cross beds, and horizontal burrows within the deposits. For additional details on the ichnology of tidal deposits, readers are referred to Chap. 4.

13.7 Transgressive Stratigraphy

As noted already, sandy tidal deposits on modern shelves are transgressive in origin (Fig. 13.20), and such is likely to be the case in the ancient as this is the main time that coarse-grained sediment (coarser than mud) is able to escape from nearshore areas onto the shelf. The siliciclastic sand that forms these deposits is derived primarily from the reworking of older deposits, including such features as drowned valley fills (Reynaud et al. 1999c), lowstand deltas (Posamentier 2002; Berné et al. 2002; Fig. 13.21) and transgressed coastal barriers (Fig. 13.6a). Sand is especially abundant seaward of headlands, because the convergence of longshore drift, coupled with erosional retreat of the shoreline, creates a large headland-attached sand body called a *shoal retreat massif* (Swift 1975). Similar sediment bodies also form seaward of river mouths. As the transgression progresses and the shoreline migrates landward, nearshore ridges become left behind on the shelf where they can either become moribund or continue to be reworked actively. Even where the source deposit is muddy, the tidal currents can winnow away the mud and produce a sandy deposit, as illustrated by some ridges in the East China Sea (Liu et al. 2007).

Erosion of the shoreline and shelf during the transgression is generally termed *transgressive ravinement*. In wave-dominated settings, transgressive ravinement is generally limited to the shoreface, forming a wave ravinement surface. In tidal environments, transgressive ravinement occurs at the coast, both as tidal ravinement at river mouths and as wave ravinement

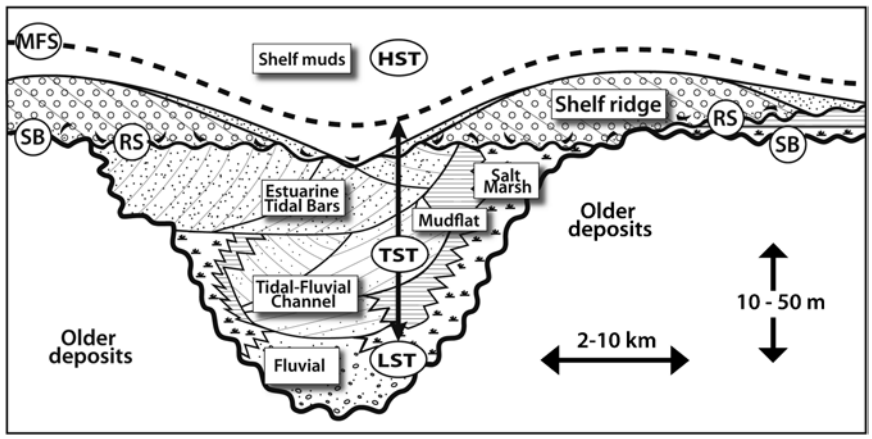

Fig. 13.20 Model of depositional succession on transgressive tidal shelves, supposing that all of the facies tracts are superimposed on each other. The succession begins with a valley-fill deposit that is capped by tidal-current ridges that formed on the shelf. *LST*, *TST*, *HST* lowstand, transgressive, and highstand systems tracts; *SB* sequence boundary; *RS* transgressive ravinement surface; *MFS* maximum flooding surface (After Dalrymple 2010b)

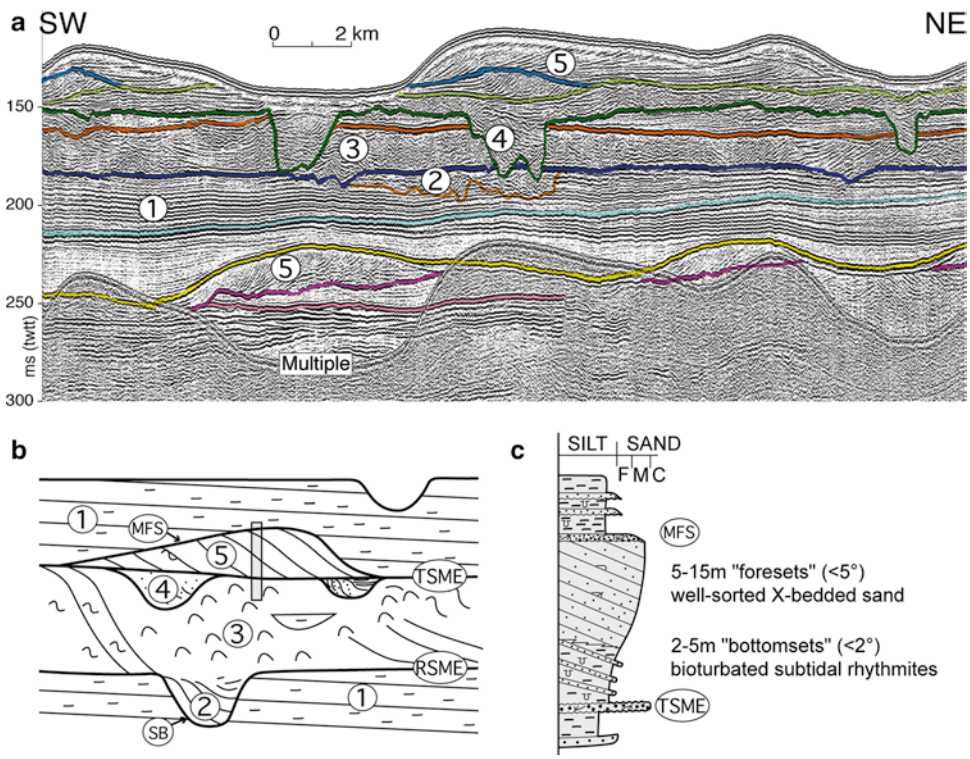

Fig. 13.21 (**a**) Seismic section from the East China Sea, offshore from the Changjiang River (see location in Fig. 13.6b, ridge field 2). Laterally migrating tidal ridges are present on the modern surface; older ridges are present near the bottom of the section, buried beneath prodeltaic mud. (**b**) Interpretation of the succession, as determined from seismic attributes and facies in cores. Depositional environments in (**a**) and (**b**): *1* prodeltaic deposits, *2* deltaic/estuarine channels of the falling-stage and lowstand systems tracts, *3* fluvial deposits of the lowstand systems tract, *4* early transgressive estuarine channels, and *5* transgressive shelf ridges. *RSME* regressive surface of marine erosion, *TSME* transgressive surface of marine erosion, *SB* sequence boundary, *MFS* maximum flooding surface. (**c**) Schematic vertical succession through the ridge (location shown by the *gray rectangle* in **b**). The coarsening-up succession reflects the increase of hydrodynamic energy toward the ridge crest. Note the coarse lag at the bottom of the ridge, which is interpreted as the tidal ravinement surface (From Berné et al. 2002)

along the open-coast shoreface. It continues, however, in the offshore area as a result of tidal scour in widespread, bedload-parting and bypass zones, forming a surface that we term an *offshore tidal ravinement surface* (Reynaud et al. 2003) to distinguish it from ravinement surfaces formed in the coastal zone. The offshore tidal ravinement surface can be continuous with the coastal ravinement surface, or can be stratigraphically distinct, as is the case where the bedload parting area migrates over areas that were formerly depositional (Fig. 13.19a).

If the sand liberated from the seafloor by offshore tidal ravinement is carried away by the residual transport, erosional offshore tidal ridges can form, as is the case in the Yellow Sea and the Korea Strait (Jung et al. 1998; Jin and Chough 2002, Park et al. 2006). The outer shape of the Celtic Banks has also been interpreted by some authors as purely erosional (Berné et al. 1998). The same circulation cells as those shown in Figure 13.8 exist, but in an erosional, rather than depositional, mode. Some of these ridges have been sculpted into muddy estuarine deposits that predate the last glacial-maximum lowstand (Fig. 13.22), and are mantled by a veneer of modern tidal sand. As sea level rises, the erosional area can migrate landward and the ridges can enter a progressively more depositional regime while current speeds decrease. A constructional tidal ridge may then develop above the erosional form that acts as the nucleus for sediment deposition. Numerous examples of offshore tidal ridges that show this erosional-depositional history exist, including the ridges of the Boulonnais along the northern French coast (Lapierre 1975; De Batist et al. 1996) and the Flemish Banks in the southern North Sea (D'Olier 1981; Laban and Schuttenhelm 1981; Berné et al. 1994; Trentesaux et al. 1999; Fig. 13.23).

Thus, extending the evolutionary model proposed by Snedden and Dalrymple (1999), there might be a continuum between erosional (juvenile) and constructional (fully evolved) ridges as conditions change over a transgression (Fig. 13.24). Juvenile ridges contain the initial relief or bump from which they grew. In some instances, this precursor might be composed of sand. This is, for example, the case of one of the Flemish Banks (Trentesaux et al. 1999; Fig. 13.23). There, the 'precursor' consists of a finer-grained, more bioturbated and less well sorted sandbody (U4 in Fig. 13.23) that may correspond to a shoreface-attached ridge,

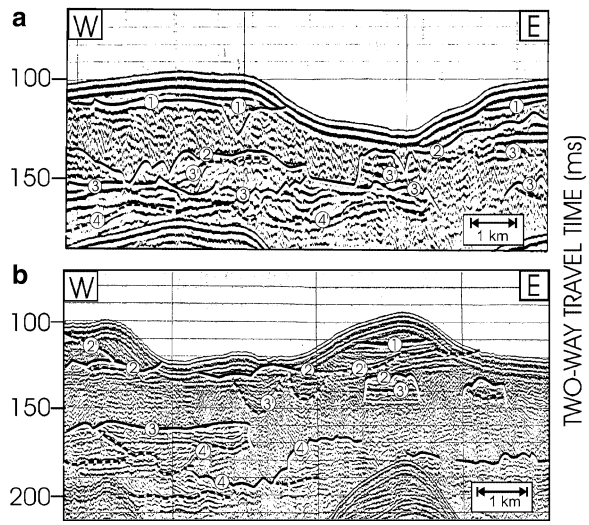

Fig. 13.22 Interpreted seismic sections showing the complex internal architecture of erosional transgressive tidal ridges in the eastern part of the Yellow Sea. The internal bedding is overall aggradational, comprising two seismic facies interpreted as lowstand, probably fluvial, deposits (chaotic reflections) that rest on sequence boundaries (circled numbers without prime), and early transgressive tidal coastal muds (stratified deposits) that rest on tidal ravinement surfaces (circled numbers with prime). The ridge shape is entirely erosional, with the external surface truncating strata within the ridge. Most of the sediment within the ridge is muddy heterolithic deposits that predate the last glacial lowstand (From Jin and Chough 2002)

resting on a pebble lag (the wave ravinement surface). This is overlain, above a prominent offshore tidal ravinement surface, by the modern shelf ridge that consists of well-sorted, coarser, bioclastic-rich crossbedded sand (U6-7 in Fig. 13.23). The longer the ridges are active, the more fully developed they are likely to become. As a consequence, the ridges that originate early in the transgression and are, thus, located on the outer shelf today, are more likely to be fully evolved than those that originated close to the highstand coast, as examplified by the ridges in the English Channel and its Western Approaches (Fig. 13.25).

As the water depth increases during the transgression, the tidal-current speeds can decrease (Fig. 13.26), causing the tidal ridges to become moribund (i.e. they are no longer active). The Celtic Ridges are the best-described examples of moribund ridges (Bouysse et al. 1976; Pantin and Evans 1984; Reynaud et al. 1999a, b). They have a rounded shape, and there is evidence of storm erosion of their crest and the development of

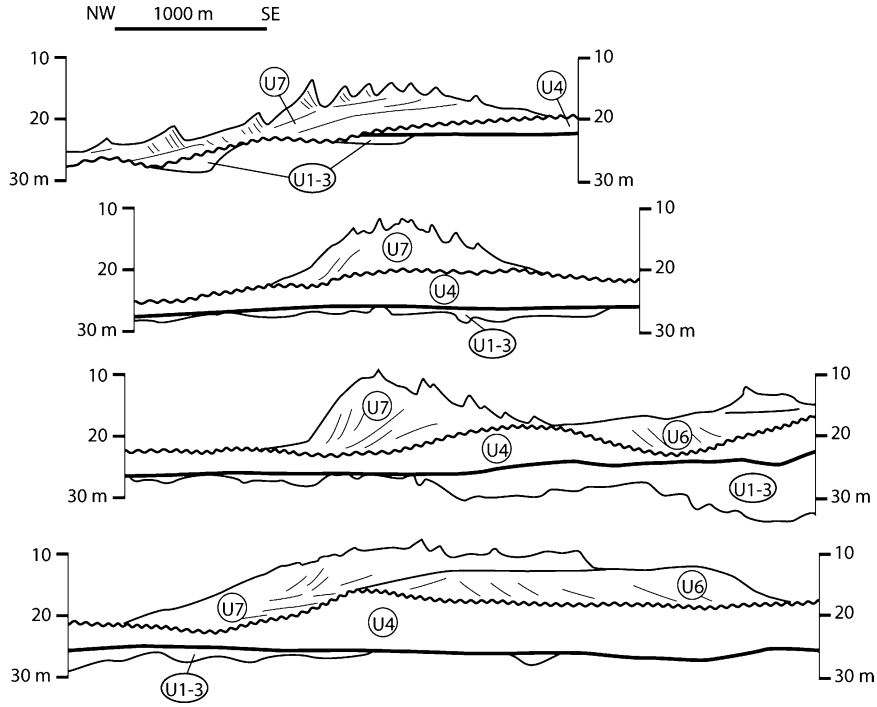

Fig. 13.23 Seismic profiles across Middelkerke Ridge (Flemish Ridges, Southern North Sea, see Fig. 13.6a). *U1–U3* estuarine channels and tidal flats; *U4* coastal barrier, shoreface and ebb-deltas; *U6–U7* active, offshore tidal ridge. The sinusoidal *bold line* is the offshore tidal ravinement surface; the clean, offshore sands of the ridges lie on this surface. The plain thick *black line* is the wave ravinement surface, which is marked by a pebble lag (After Trentesaux et al. 1999)

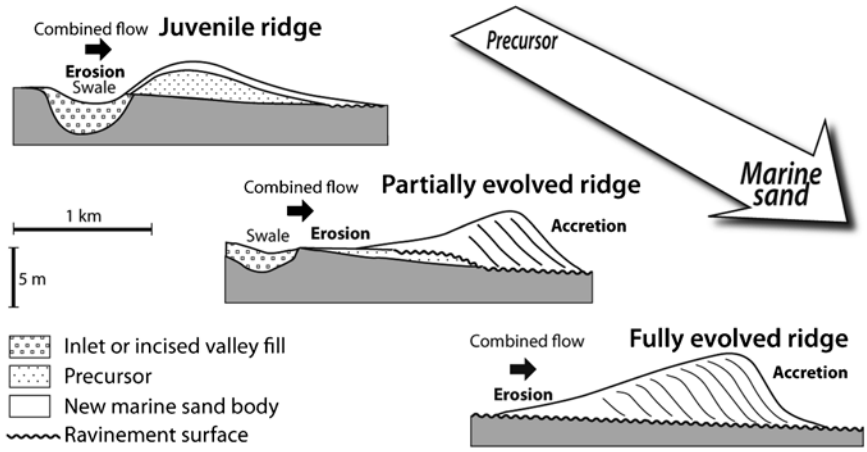

Fig. 13.24 Evolutionary model of offshore ridges. An initial bump, or nucleus, is required to start the Huthnance process. As the ridge migrates in response to the residual current, this initial core ends up being removed by erosion of the upcurrent side of the ridge. Fully developed ridges are exemplified by the deepest Norfolk Ridges in the Southern North Sea (Figs. 13.6a and 13.10). Partially evolved ridges that retain part of the original nucleus are more similar to the Flemish Ridges (Fig. 13.23) that are located closer to the coast and started to form later in the last transgression (From Snedden and Dalrymple 1999)

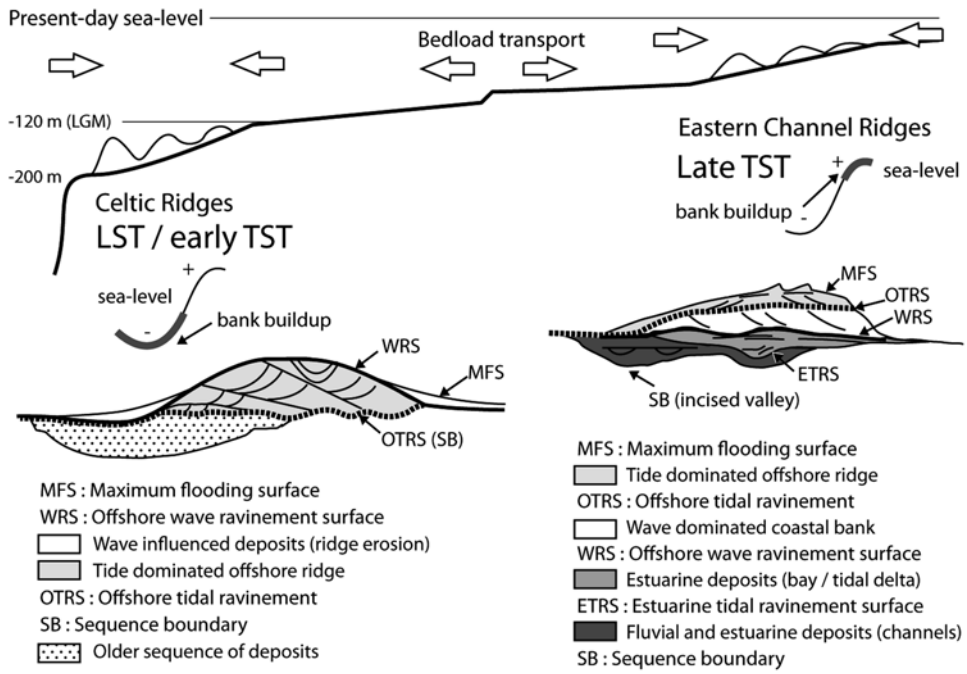

Fig. 13.25 Depositional setting and key sequence-stratigraphic surfaces within tidal sand ridges in the southern Celtic Sea and eastern English Channel (see location in Fig. 13.6a, ridge fields 6 and 4, respectively) that were formed early and late, respectively, in the last post-glacial transgression. The shallower tidal ridges have a core that may preserve coastal sandbodies. By contrast, the offshore tidal ravinement surface has more time to rework the deeper ridges, which are therefore 'fully evolved' (cf. Fig. 13.24). Subsequent to their formation, tidal currents became weaker in the course of the transgression, leaving them "moribund" and partly eroded by storm waves, forming a wave ravinement surface at their crest (After Reynaud et al. 2003)

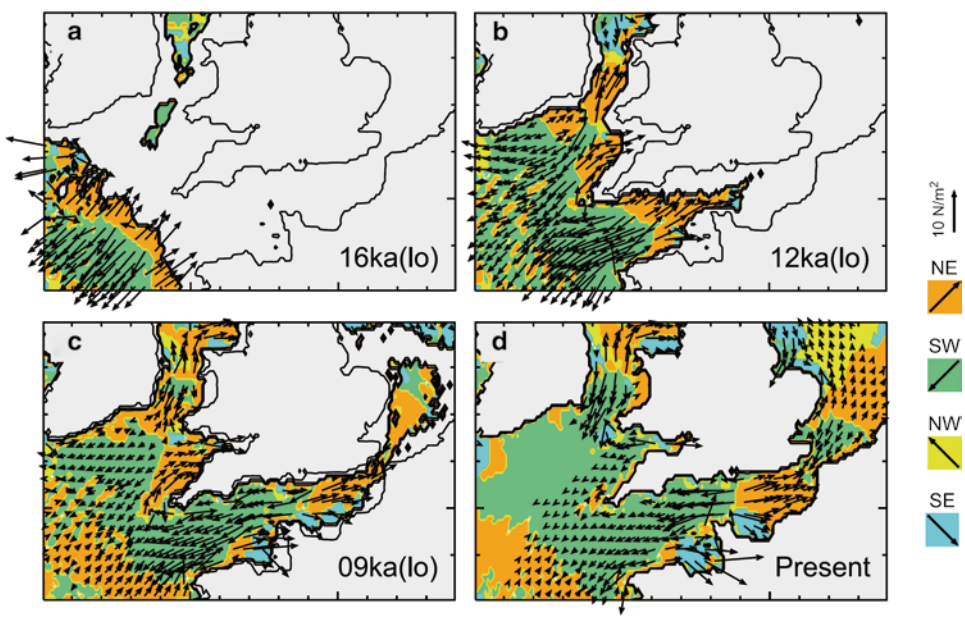

Fig. 13.26 Paleotidal modeling of the English Channel, Irish Sea and southern North Sea for four times during the last transgression. The maps show the peak bed-stress vectors (length is proportional to the current strength) and the directions of potential sand transport, which define the tidal-transport pathways that evolve through time as sea level rises. The peak bed stress near the shelf-margin, in the area occupied by the Celtic Sea sand ridges (Figs. 13.6a and 13.12), is at a maximum around 16 ka, suggesting that these ridges were formed in the early stage of the last transgression. Note that, as transgression proceeds eastward up the English Channel, the shear stress decreases until the Strait of Dover is flooded, at which time conditions are created that allow the formation of a new set of ridges there (cf. Fig. 13.25) (From Uehara et al. 2006)

wedges of sediment that partly bury the ridge flanks (Figs. 13.12 and 13.25). Consequently, their outer slopes are less steeply inclined than those of active ridges, and commonly dip at less than 1° (Stride et al. 1982). Dunes, which typically mantle active ridges, are generally absent from their crest. A decrease in the ability of the tidal currents to bring in more sand leads to an increase in the carbonate content of the sediment, forming a shelly lag on the ridge crest; the constituents present in this bioclastic material should record the increasing water depth (Wilson 1988). The increase in shell content can be either gradual or abrupt (Wilson 1982; Davis et al. 1993). The surface of the ridge can also become pervasively bioturbated. In the ancient, the post-ridge draping deposits might record a transition from tidal to wave dominance, as reported from examples in the Western Interior Cretaceous of the USA (Hein et al. 1991; Mellere and Steel 1995; Yoshida et al. 2007). As would be expected in a transgressive succession (Fig. 13.20), the first deposits above the ridge crest are glauconitic shelf muds that indicate sediment starvation and slow sedimentation (Surlyk and Noe-Nygaard 1991) and the formation of the maximum flooding surface. The dominantly muddy sedimentation that characterizes the overlying highstand systems tract may entirely bury the remnant ridges, as is observed in the Pleistocene of the East China Sea (Berné et al. 2002; Fig. 13.21) and the Miocene of offshore Java (Posamentier 2002).

13.8 Sea-Level and Geomorphic Interactions

Because the oceanic tidal wave interacts strongly with the morphology of the shelf and coastline, changes in the geomorphology of an area as a result of changes in relative sea level can have a profound influence on the occurrence of tidal deposits. As noted above, it is generally believed that the formation of *sandy* tidal-shelf deposits is restricted to transgressive situations. The occurrence of *muddy* tidal-shelf deposits is not well known because they have not been studied as systematically, but they appear to occur mainly in regressive, delta-related settings (e.g. the Amazon River: Gabioux et al. 2005; Bourret et al. 2008; the Irrawaddy River: Viana et al. 1998; Ramaswamy et al. 2004; Rao et al. 2005; the Yellow River: Yang and Liu 2007). Such deposits are discussed elsewhere in this volume (Chap. 7). From a theoretical point of view, however, there is no reason for tidal dominance to occur only during transgressions (Yoshida et al. 2007). The following sections explore the timing of tidal dominance, focusing primarily on the results of paleotidal modeling of both modern and ancient basins.

13.8.1 High-Frequency Changes

Short-term, tectonic- or climate-driven sea-level variations with a period of less than about 100,000 years (fourth-order or higher; Vail et al. 1977) can bring about rapid change in the nature of shelf sedimentation, potentially causing an alternation between tidal and non-tidal deposits (Fig. 13.21). Two contrasting situations can be documented: (i) open shelves on passive margins, and (ii) epicontinental seaways.

On open shelves, the tidal influence is expected to increase with rising sea level, because the increasing shelf width typically brings the system closer to resonance, although the opposite can occur if the width at lowstand is close to one-quarter of the tidal wavelength. If the shelf has embayments, they might be the most sensitive to changes in tidal influence, due to funneling of the flow toward the head of the bay. The increase in tidal influence can be geologically instantaneous in situations where the geomorphology changes rapidly. This was the case in the Gulf of Maine-Bay of Fundy system, which changed from microtidal to extreme macrotidal over a period on only a few thousand years (Greenberg 1979; Dalrymple and Zaitlin 1994; Shaw et al. 2010). One possible ancient analogue is provided by the Woburn Sands in the Cretaceous Greensand Seaway of NW Europe, where the strength of the tides increases upward through the transgressive succession, being stronger in shelf sediments than it is in estuarine deposits at the base (Yoshida et al. 2004), a situation that is the reverse of what might be expected because tidal currents are typically stronger within embayments than on the open shelf. Once tidal resonance has been reached, however, any further increase in sea level will result in the decrease in tidal influence. This might be illustrated by the sudden abandonment and preservation of fossil tidal dune fields beneath Holocene offshore muds in the Southern North Sea (Brew 1996). This could also be the case for the tidal sandbodies of the Devonian Castkill Sea (Ericksen et al. 1990).

It must be noted that different parts of the transgressing sea can become resonant at different times, or

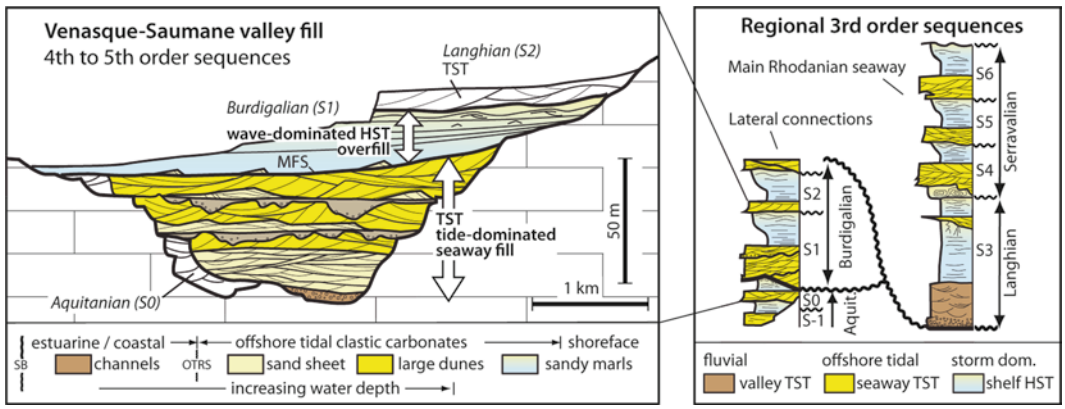

Fig. 13.27 Succession of deposits in the Miocene foreland-basin seaway of SE France, showing the influence of changing sea level and morphology on the development of tidal deposits. (*Right*) Succession of third-order sequences (S1–S6), each of which is composed of a lower, bioclastic-rich transgressive (*TST*) deposit formed by tidal dunes, and an upper marly, wave-influenced highstand (*HST*) deposit. The sequence boundaries are possibly subaerial erosion surfaces, but they were intensely scoured by strong tidal currents during transgression, forming tidal ravinement surfaces. The thickness of the sequence set exceeds 100 m in most places. (*Left*) Detailed architecture of the Saumane-Venasque seaway filled and overtopped by sequence S1. When relative sea level was low and water was confined to the valley, the deposits were tide-dominated, coarse-grained bioclastic material. Once the water level rose above the interfluves, the cross-sectional area increased dramatically, so that tidal-current strength decreased, and the deposits became fine grained and wave-dominated. *OTRS* offshore tidal ravinement surface. This depositional pattern is repeated in each of the six sequences shown in the *right-hand* figure (After Besson 2005 and Besson et al. 2005)

perhaps more than once during a major transgression. This might have been the case for the English Channel during the last sea-level rise. After a first 'tidal climax' early in the post-glacial transgression (i.e., at ca. 16 ka BP), an abrupt loss of tidal resonance was recorded that might correspond to the end of active up-building of the Late Pleistocene Celtic Banks (Reynaud et al. 1999b; Uehara et al. 2006). Much more recently, a second phase of strong tidal action has occurred in the Normandy-Brittany Gulf and Eastern Channel, bringing about the formation of a second set of tidal ridges at a much more landward location (Reynaud et al. 2003; Fig. 13.25).

In the case of broad seaways, the tidal influence is likely to increase with falling sea level, because narrowing of the seaways favors the constriction of tidal flows and restricts the fetch of wind waves (Yoshida et al. 2007). A narrowing of the seaway due to progradation of its margins would have the same effect, even if water depths were increasing (Van der Molen et al. 2004). The Cretaceous Western Interior Seaway of Northern America provides examples of this type of response to sea-level change, with lowstand deposits being tide-dominated, whereas highstand deposits are wave-dominated (see Chap. 17). In a different example, paleotidal modeling by Wells et al. (2007) showed that tidal circulation inside the Late Pennsylvanian Midcontinent Seaway of America would have been diminished during times of maximum flooding, promoting the development of black shales, whereas the lowstand to transgressive intervals, when the seaway was narrower, favored the development of large tides in the eastern embayment of the seaway, as recorded by the coeval fluvial-estuarine transition in Kansas (Lanier et al. 1993). At a smaller scale, the same interpretation is provided by the Miocene incised valleys/seaways of SE France (Besson et al. 2005; Reynaud et al. 2006). During highstands, the valley interfluves are flooded creating broad seaways in which deposition consisted of wave-influenced carbonate-rich mudstones with minimal tidal influence (Fig. 13.27). By contrast, when sea level fell and the interfluves became emergent, flow constriction within the valleys lead to the accumulation of localized tide-dominated deposits. Other examples of water-depth control on the strength of tidal currents in seaways are provided by Anastas et al. (2006; Oligocene of New Zealand) and Surlyk and Noe-Nygaard (1991; Jurassic of Scotland; Fig. 13.28).

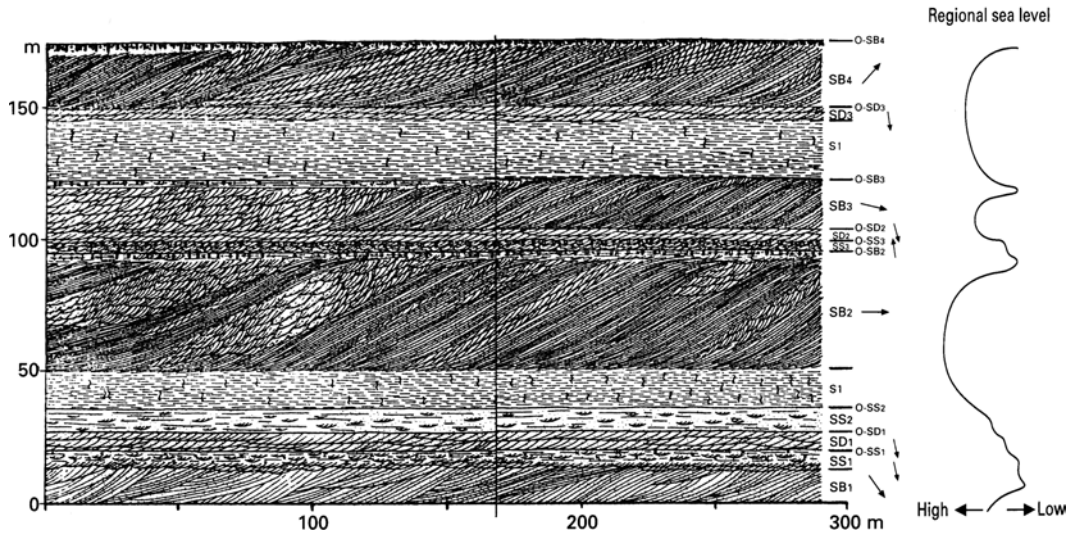

Fig. 13.28 Inferred influence of sea-level change on the architecture of tidal deposits infilling a Jurassic seaway that occupied a North Sea rift basin. The succession consists of an alternation of thick crossbedded deposits formed by large dunes migrating along the axis of the seaway that form a tidal sand ridge during transgressive periods, and finer-grained and more thinly bedded sandstones that accumulated during highstands when the water depth was greater and the currents speeds were less. Each sea-level fall and the start of the subsequent transgression is marked by a discrete pebble lag and bioturbated, glauconitic horizon that underlies the giant crossbeds. Labels in the margin refer to deposit attributes (*SB* sand bank, *SS* sand sheet, *arrows* palaeocurrents) (From Surlyk and Noe-Nygaard 1991)

13.8.2 Long-Term Changes in Basin Morphology

On the much longer time scale of first- to second-order sea-level changes (up to a few hundreds of meters of relative sea-level change, stretching over tens to hundreds of millions of years), two generic end-member situations arise (Fig. 13.29). During overall low sea-level periods (e.g. during the late Cenozoic and present), there is limited flooding of continental interiors. Most shallow-marine sedimentation occurs on narrow shelves at the margins of the continents. Large-scale embayments are restricted primarily to tectonically structured seaways along collisional or transform margin (Kamp et al. 1988; Hoppie 1996). During overall high sea level, such as in the Upper Cretaceous, by contrast, a much larger part of the continents is flooded, creating extensive semi-enclosed seas with a complex topography. Because of their complex paleogeography, these seas experience very complex interactions between friction forces and tide-enhancing processes that cannot be solved without the help of paleotidal modeling.

It is expected that, in the course of an overall first- or second-order transgression, the shelf will gradually grow wider, with the progressive development of a more complex coastline, including tidal embayments that can extend many hundreds of kilometers inland (Houbolt 1982; Houthuys and Gullentops 1988a, b; André et al. 2003). With continued sea-level rise, these embayments can eventually evolve into tidal seaways and straits with a marine connection at both ends (e.g. Anastas et al. 1997; Besson et al. 2005; Longhitano and Nemec 2005). Whereas tidal currents must decrease at the head of an embayment, they can be accelerated through a seaway, making possible the propagation of a progressive tidal wave and the maintenance of strong tidal currents a long distance into the continental interior. This seems to have been the case for the Peri-Alpine, Miocene seaway of southern Europe, which formed a short-lived connection between the Atlantic and the Paratethys during the Burdigalian (Allen et al. 1985; Martel et al. 1994; Bieg 2005; Fig. 13.30). If, however, tidal resonance occurs at the embayment stage, the connection of the head of the embayment to another tidal basin as a

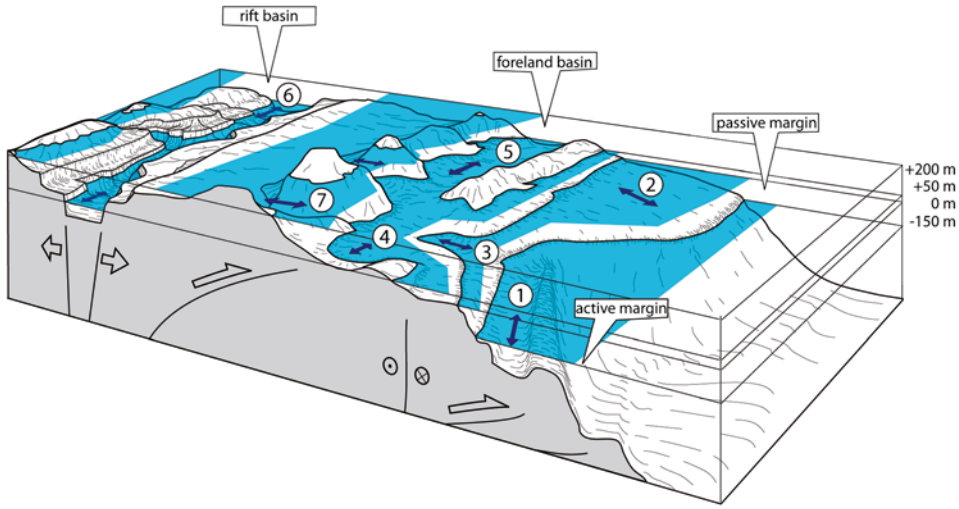

Fig. 13.29 Schematic diagram showing the range of tectonic basin types. In each type, changes in relative sea level cause a change in basin morphology, which in turn controls where and when tidal deposits will form. The *arrows* are oriented parallel to the mean tidal current. The flooding levels displayed correspond to the extremes of long-term (first or second order), high-amplitude sea-level cycles. Drawing not to scale. Active and passive margins are displayed as adjacent to each other only for convenience. Examples: *1*– Te Kuiti Group, New Zealand, Oligocene (Anastas et al. 1997, 2006); Hikurangi fore-arc basin, New Zealand, Pliocene (Kamp et al. 1988; Nelson et al. 2003); Cuyama transform margin, California, Miocene (e.g. Hoppie 1996). *2* Celtic Sea, Late Pleistocene (e.g. Bouysse et al. 1976); South China Sea, Late Pleistocene (e.g. Berné et al. 2002). *3* English Channel, Late Pleistocene to Holocene (e.g. Reynaud et al. 2003). *4* Southern North Sea, Holocene (e.g. Berné et al. 1994; Trentesaux et al. 1999); Yellow Sea, Holocene (e.g. Park et al. 2006); Greensand Seaway, Aptian (Yoshida et al. 2004; Wells et al. 2010). *5* Perialpine Seaway, Burdigalian (e.g. Lesueur et al. 1988; Bieg 2005). *6* North Sea rift basin (Scotland), Jurassic (Blackwood et al. 2004; Mellere and Steel 1996). *7* Bohemian Basin, Turonian (e.g. Mitchell et al. 2010). In *1*, *5*, *6* and *7*, the main control on tidal sedimentation is the constriction of the tidal flow through a narrow passageway. The tidal range does not need to be large. In *2*, *3* and *4*, the main control is the increase in tidal amplitude, related to either an increase in tidal prism (embayments) and/or tidal resonance (shelf)

result of sea-level rise could bring about an abrupt decay of tidal currents, as demonstrated by the postglacial evolution of Cook Strait, New Zealand (Proctor and Carter 1989). As a result of paleotidal modeling of the Lower Cretaceous Greensands Seaway in Europe, Wells et al. (2010) suggest that, although the southern connection of the seaway to the Neotethys would have been crucial for the development of significant tides, the existence of a coeval connection to the North Sea would have caused tides to decrease (Fig. 13.31).

During times of very high sea level and extensive flooding of the continents, extensive, shallow-marine carbonate sedimentation would occur around emergent archipelagos. Paleotidal modeling shows that such a broad, shallow platform would probably be microtidal, due to the great distance from the open ocean. In such a setting, strong tidal currents would occur only within small constrictions between islands, as shown by modeling of the Bohemian Cretaceous Basin (Mitchell et al. 2010), or of the Lower Jurassic Laurasian Seaway (e.g. Luxembourg sandstones, P. Allison 2010, personal communication).

13.9 Summary

The astronomic tide that exists in the deep ocean basin is amplified as it propagates onto the continental shelf, and is transformed into a co-oscillating tide by complex interactions with the shallow-water topography. Particularly pronounced tidal currents occur where there is tidal resonance in embayments and where there is local enhancement of tidal currents by a flow constriction as in seaways. Tidal currents are efficient in transporting sediments up to medium-grained sand to

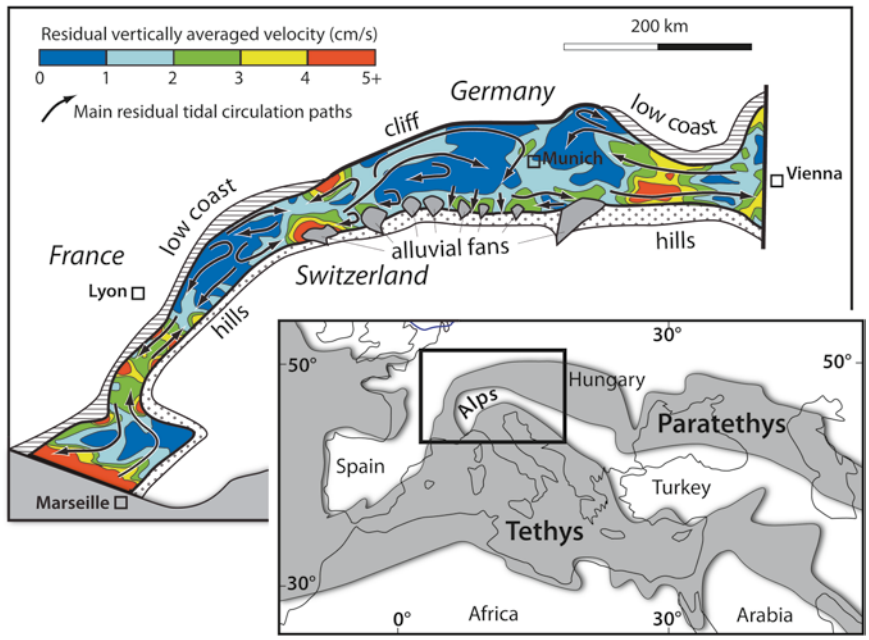

Fig. 13.30 Paleotidal modeling of the Burdigalian Peri-Alpine Seaway. The colors show the velocity of residual tidal circulation and the arrows the tidal-transport pathways. The first paleotidal modeling of this system by Martel et al. (1994) demonstrated that the Swiss Molasse basin, which hosts offshore tidal deposits, would have been meso- to macrotidal only if the tidal wave entered the seaway from both the southwest and eastern ends. More recent work by Bieg (2005) showed that the two tidal waves had to be in phase to get the maximum resonance. The numerically determined current patterns and strengths show a relatively good agreement with the facies distribution and tidal-transport pathways reconstructed from the bedforms in SE France (e.g. Lesueur et al. 1988), Switzerland (e.g. Homewood and Allen 1981), Germany (e.g. Hülsemann 1955) and Hungary (e.g. Sztano and de Boer 1995) (After Bieg 2005). *Inset* map modified from Martel et al. 1994)

depths of approximately 200 m. These currents can deposit large accumulations of well-sorted sand over large areas, and are responsible for the resuspension and redistribution large amounts of mud.

Interactions between various components of the tide, and with the seafloor and coastal morphology, cause the ebb and flood tidal currents to be unequal over large areas. These inequalities generate tidal-transport pathways along which bedload can be transported for distances of tens to hundreds of kilometers, from high-energy erosional and by-pass zones, to lower energy areas of sediment accumulation. The sandy tidal sediments that accumulate in offshore areas are commonly coarser and less muddy than those deposited at equivalent depths on storm-influenced shelves.

The most significant offshore tidal sediment accumulations are sand sheets and ridges. These deposits are made up predominantly of the crossbedded sandstone formed by tidal dunes, which can reach more than 10 m in height. Most of these bedforms are compound dunes, and generate compound crossbedding in which a single the master bedding and smaller cross beds dip in the direction of the residual transport. Herringbone crossbedding can be present in small amounts, but mud drapes, reactivation surfaces and tidal bundles are not likely to be abundant. The ichnology of these deposits reflects the mobile sandy nature of the deposits, and the normal-marine salinity of the water.

Most sandy tidal-shelf deposits are transgressive in origin, with the sand supplied by erosion of the retreating coast or the offshore bedload parting area, and can rest on an offshore tidal ravinement surface that commonly cuts into older coastal deposits. This scour surface can be amalgamated with a sequence boundary, or can be a more prominent distinct surface. The upper boundary of the offshore tidal deposit is expected to be a maximum flooding surface that reflects the decay of tidal currents in the course of a sea-level rise. The large size of some tidal dunes and tidal-current ridges means

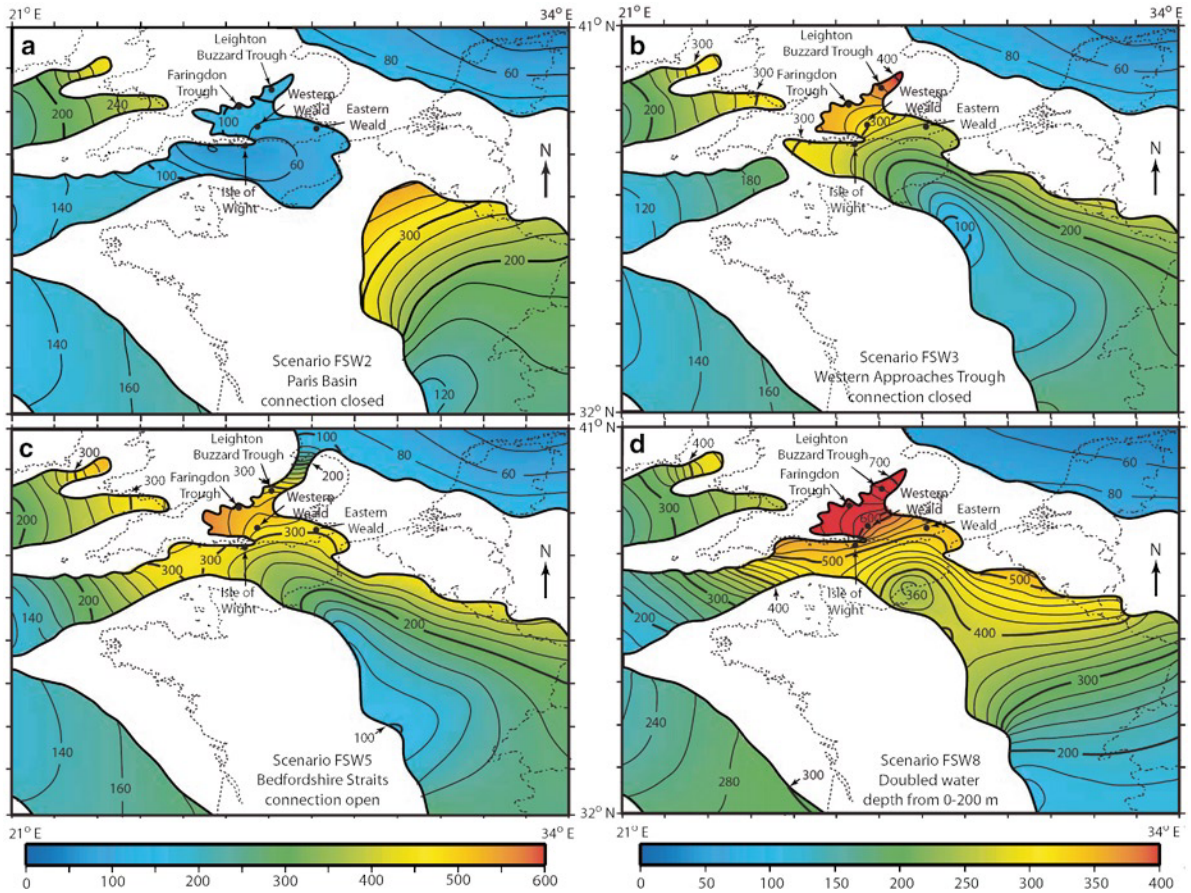

Fig. 13.31 Paleotidal modeling of the Lower Cretaceous seaways of Western Europe. Color bar at the bottom gives the modeled tidal range. Several paleogeographic hypotheses, based on field data of the Greensand Seaway in southern Great Britain and northern France, are compared: (**a**) seaway connected only to the North Atlantic; (**b**) seaway connected only to the Neotethys; (**c**) all three connections open; and (**d**) Neotethys and North Atlantic connections open, and water depth doubled in the areas shallower than 200 m. The results show that (i) only the Neotethys connection was important for the transfer of tidal energy into the seaway (i.e. there is a significant tidal range only when the Neotethys connection is open (**b**, **c** and **d**), and (ii) the tidal range increases when sea level is higher (From Wells et al. 2010)

that original topographic relief may be preserved on the top of offshore tidal deposits.

Shelf tidal sedimentation can, however, occur at any time during a relative sea-level cycle, whenever the sea level interacted with the paleogeography to create embayments and straits that accentuated the tidal currents. Changes in coastal and shelf morphology that result from a change in relative sea level can cause dramatic changes in the strength of the tidal currents on rapid time scales. Paleotidal modeling has great potential to assist in understanding the complex temporal and spacial occurrence of shallow-marine tidal deposits in the rock record.

References

Allen JRL (1980) Sand waves; a model of origin and internal structure. Sediment Geol 26:281–328

Allen JRL (1982) Sedimentary structures: their character and physical basis, Developments in sedimentology 30A and 30B. Elsevier, Amsterdam

Allen PA (1997) Earth surface processes. Wiley-Blackwell, Oxford

Allen PA, Homewood P (1984) Evolution and mechanics of a Miocene tidal sandwave. Sedimentology 31:63–81

Allen PA, Mange-Rajetzky M, Matter A, Homewood P (1985) Dynamic palaeogeography of the open Burdigalian seaway, Swiss Molasse basin. Eclogae Geol Helv 78:351–381

Anastas A, Dalrymple RW, James NP, Nelson CS (1997) Cross-stratified calcarenites from New Zealand; subaqueous dunes

in a cool-water, Oligo-Miocene seaway. Sedimentology 44:869–891

Anastas A, Dalrymple RW, James NP, Nelson CS (2006) Lithofacies and dynamics of a cool-water carbonate seaway; mid-Tertiary, Te Kuiti Group, New Zealand. In: Pedley HM, Carannante G (eds) Cool-water carbonates: depositional systems and palaeoenvironmental controls. Geol Soc Lond Spec Publ 255:245–268

André JP, Biagi R, Moguedet G, Buffard R, Clément G, Redois F, Baloge PA (2003) Mixed siliciclastic–cool-water carbonate deposits over a tide-dominated epeiric platform: the Faluns of l'Anjou formation (Miocene, W. France). Ann Paleontol 89:113–123

André JP, Barthet Y, Ferrandini M, Ferrandini J, Reynaud JY, Tessier B (2011) The Bonifacio Formation (Miocene of Corsica): transition from a wave- to tide-dominated coastal system in mixed carbonate-siliciclastic setting. Bull Soc Geol France 182:221–230

Androsov AA, Kagan BA, Romanenkov DA, Voltzinger NE (2002) Numerical modeling of barotropic tidal dynamics in the strait of Messina. Adv Water Res 25:401–415

Archer AW, Hubbard MS (2003) Highest tides of the world. In: Chan MA, Archer AW (eds) Geol Soc Am Spec Paper 370:151–173

Ashley GM (1990) Classification of large-scale subaqueous bedforms: a new look at an old problem. J Sediment Petrol 60:160–172

Bassant P, Van Buchem FHP, Strasser A, Gorur N (2005) The stratigraphic architecture and evolution of the Burdigalian carbonate-siliciclastic sedimentary systems of the Mut Basin, Turkey. Sediment Geol 173:187–232

Bastos AC, Collins M, Kenyon NH (2003) Morphology and internal structure of sand shoals and sandbanks off the Dorset coast, English Channel. Sedimentology 50:1105–1122

Belderson RH, Johnson MA, Kenyon NH (1982) Bedforms. In: Stride AH (ed) Offshore tidal sands: processes and deposits. Chapman & Hall, London

Berné S, Auffret J-P, Walker P (1988) Internal structure of subtidal sandwaves revealed by high-resolution seismic reflection. Sedimentology 35:5–20

Berné S, Bourillet J-F, Durand J, Lericolais G (1989) Les Dunes subtidales geantes de Surtainville (Manche ouest). Bull Cen Rech Expl Elf-Aquit 13:395–415

Berné S, Durand J, Weber O (1991) Architecture of modern subtidal dunes (sand waves), Bay of Bourgneuf, France. Concepts Sedimentol Paleontol 3:245–260

Berné S, Trentesaux A, Stolk A, Missiaen T, De Batist M (1994) Architecture and long term evolution of a tidal sandbank; the Middelkerke Bank (southern North Sea). Mar Geol 121:57–72

Berné S, Lericolais G, Marsset T, Bourillet J-F, de Batist M (1998) Erosional shelf sand ridges and lowstand shorefaces: examples from tide and wave dominated environments of France. J Sediment Res 68:540–555

Berné S, Vagner P, Guichard F, Lericolais G, Liu Z, Trentesaux A, Yin P, Yi HI (2002) Pleistocene forced regressions and tidal sand ridges in the East China Sea. Mar Geol 188:293–315

Besson D (2005) Architecture du bassin rhodano-provençal miocène (Alpes, SE France): relations entre déformation, physiographie et sédimentation dans un bassin molassique d'avant-pays. Ph.D. thesis, Mines Paris Tech

Besson D, Parize O, Rubino J-L, Aguilar J-P, Aubry M-P, Beaudoin B, Berggren WA, Clauzon G, Crumeyrolle P, Dexcoté Y, Fiet N, Iaccarino S, Jimenez-Moreno G, Laporte-Galaa C, Michaux J, von Salis K, Suc J-P, Reynaud J-Y, Wernli R (2005) Un réseau fluviatile d'âge Burdigalien terminal dans le Sud-Est de la France: remplissage, extension, âge, implications. CR Géosci 337:1045–1054

Bieg U (2005) Palaeoceanographic modeling in global and regional scale: an example from the Burdigalian Seaway Upper Marine Molasse (Early Miocene). Ph.D. thesis, University of Tübingen

Blackwood S, Yoshida S, Steel R, Dalrymple R, Martinius A, Gawthorpe R (2004) Comparative studies of modern, Quaternary and ancient seaways; building depositional models for hydrocarbon exploration and production; a review. AAPG Abstr 13:14–15

Bourret A, Devenon J-L, Chevalier C (2008) Tidal influence on the hydrodynamics of the French Guiana continental shelf. Cont Shelf Res 28:951–961

Bouysse P, Horn R, Lapierre H, Le Lann F (1976) Etude des grands bancs de sable du Sud-est de la mer Celtique. Mar Geol 20:251–275

Bouysse P, Le lann F, Scolari G (1979) Les sediments superficiels des Approches occidentales de la Manche. Mar Geol 29:107–135

Brandano M, Jadoul F, Lanfranchi A, Tomassetti L, Berra F, Ferrandini M, Ferrandini J (2009) Stratigraphic architeture of mixed carbonate-siliciclastic system in the Bonifacio Basin (Early-Middle Miocene, South Corsica). Excursion guidebook, 27th IAS meeting of sedimentology, Alghero, 20–24 Sept 2009, pp 299–313

Brew DS (1996) Late Weichselian to early Holocene subaqueous dune formation and burial off the North Sea Northumberland coast. Mar Geol 134:203–211

Carling PA (1999) Subaqueous gravel dunes. J Sediment Res 69:534–545

Caston VND (1972) Linear sand banks in the southern North Sea. Sedimentology 18:63–78

Caston VND (1981) Potential gain and loss of sand by some sand banks in the Southern Bight of the North Sea. Mar Geol 41:239–250

Colella A (1990) Active tidal sand waves at bathyal depths observed from submersible and bathysphere (Messina Strait, southern Italy). In: 13th IAS congress, Abstract, Nottingham, pp98–99

Dalrymple RW (1984) Morphology and internal structure of sand waves in the Bay of Fundy. Sedimentology 31: 365–382

Dalrymple RW (2010a) Introduction to siliciclastic facies models. In: James NP, Dalrymple RW (eds) Facies models 4. Geological Association of Canada, St John's, pp 59–72

Dalrymple RW (2010b) Tidal depositional systems. In: James NP, Dalrymple RW (eds) Facies models 4. Geological Association of Canada, St John's, pp 201–231

Dalrymple RW, Rhodes RN (1995) Estuarine dunes and bars. In: Perillo GME (ed) Geomorphology and sedimentology of estuaries. Elsevier, Amsterdam

Dalrymple RW, Zaitlin BA (1994) High-resolution sequence stratigraphy of a complex, incised valley succession, the Cobequid Bay- Salmon River estuary, Bay of Fundy, Canada. Sedimentology 41:1069–1091

Davis RA, Balson PS (1992) Stratigraphy of a North Sea tidal sand ridge. J Sediment Petrol 62:116–121

Davis RA, Klay J, Jewell P (1993) Sedimentology and stratigraphy of tidal sand ridges, Southwest Florida inner shelf. J Sediment Petrol 63:91–104

De Batist M, Tessier B, Marsset T, Reynaud J-Y, Dimitropoulos D, Llopart X, Proust J-N, Berné S, Chamley H (1996) Analysis by geosonic recordings of the large and small-scale internal structure of the Bassure de Baas sand in the English Channel. In: Heyse I, De Moor G (eds) MAST-II-Starfish Project MAS2-CT92-0029. Final report, Chap. 15

De Boer PL, Van Gelder A, Nio SD (1988) Tide-influenced sedimentary environments and facies. Reidel Publishing, Dordrecht

Descote PY (2010) Relations architecturales, faciologiques et diagénétiques des carbonates bioclastiques du bassin rhodano-provençal (SE France). Ph.D. thesis, Mines Paris-Tech

D'Olier B (1981) Sedimentary events during Flandrian sea-level rise in the south-west corner of the North Sea. In: Nio SD, Schuttenhelm RTE, Van Weering TjCE (eds) Holocene marine sedimentation in the North Sea basin. IAS Spec Publ 5:221–227

Dyer KR, Huntley DA (1999) The origin, classification and modelling of sand banks and ridges. Cont Shelf Res 19: 1285–1330

Ekdale AA, Bromley RG, Pemberton SG (1984) Ichnology: the use of trace fossils in sedimentology and stratigraphy. SEPM Short Course Notes 15

Ericksen MC, Masson DS, Slingerland R, Swetland DW (1990) Numerical simulation of circulation and sediment transport in the late Devonian Catskill Sea. In: Cross TA (ed) Quantitative dynamic stratigraphy. Prentice-Hall, Englewood Cliffs

Fenster MS, Fitzgerald DM, Bohlen WF, Lewis RS, Baldwin CT (1990) Stability of giant sand waves in eastern Long Island Sound, U.S.A. Mar Geol 91:207–225

Fleming RH, Revelle R (1939) Physical processes in the ocean. In: Trask PD (ed) Recent marine sediments. A symposium. Thomas Murby Publishing, London

Flemming BW (1988) Pseudo-tidal sedimentation in a non-tidal shelf environment; Southeast African continental margin. In: De Boer PL, Van Gelder A, Nio SD (eds) Tide-influenced sedimentary environments and facies. Reidel Publishing, Dordrecht

Flemming BW (1980) Sand transport and bedform patterns on the continental shelf between Durban and Port Elizabeth (Southeast African continental margin). Sediment Geol 26:179–205

Gabioux M, Vinzon SB, Palva AM (2005) Tidal propagation over fluid mud layers on the Amazon shelf. Cont Shelf Res 25:113–125

Gao S, Collins MB, Lanckneus J, De Moor G, Van Lancker V (1994) Grain size trends associated with net sediment transport patterns; an example from the Belgian continental shelf. Mar Geol 121:171–185

Greenberg DA (1979) A numerical model investigation of tidal phenomena in the Bay of Fundy and Gulf of Maine. Mar Geol 2:161–187

Grochowski NTL, Collins MB, Boxall SR, Salomon J-C (1993) Sediment transport predictions for the English Channel, using numerical models. J Geol Soc Lond 150:683–695

Harris PT (1988) Sediments, bedforms, and bedload transport pathways on the continental shelf adjacent to Torres Strait, Australia – Papua New Guinea. Cont Shelf Res 8:979–1003

Harris PT, Pattiaratchi CB, Collins MB, Dalrymple RW (1995) What is a bedload parting? In: Flemming BW, Bartoloma A (eds) Tidal signatures in modern and ancient sediments. IAS Spec Publ 24 :2–10

Heathershaw AD, New AL, Edwards PD (1987) Internal tides and sediment transport at the shelf break in the Celtic Sea. Cont Shelf Res 7:485–517

Hein FJ, Robb GA, Wolberg AC, Longstaffe FJ (1991) Facies descriptions and associations in ancient reworked (transgressive) shelf sandstones; Cambrian and Cretaceous examples. Sedimentology 38:405–431

Hoppie BW (1996) The influence of relative sea level on nearshore sedimentary processes in a transform margin basin; the Miocene Cuyama Basin, California. AAPG Absr 5:67

Homewood P, Allen PA (1981) Wave-, tide- and current-controlled sandbodies of Miocene Molasse, western Switzerland. Am Assoc Petrol Geol Bull 65:2534–2545

Houbolt JJHC (1968) Recent sediments in the Southern Bight of the North Sea. Geol Mijn 47:245–273

Houbolt JJHC (1982) A comparison of recent shallow marine tidal sand ridges with Miocene sand ridges in Belgium. In: Scrutton RA, Talwani M (eds) The ocean floor, Bruce Heezen commemorative volume. Wiley, Chichester

Houthuys R, Gullentops F (1988a) The Vlierzele Sands (Eocene, Belgium): a tidal ridge system. In: de Boer PL, van Gelder A, Nio SD (eds) Tide-influenced sedimentary environments and facies. Reidel Publishing, Dordrecht

Houthuys R, Gullentops F (1988b) Tidal transverse bars building up a longitudinal sand body (middle Eocene, Belgium). In: de Boer PL, van Gelder A, Nio SD (eds) Tide-influenced sedimentary environments and facies. Reidel Publishing, Dordrecht

Houthuys R, Trentesaux A, De Wolf P (1994) Storm influences on a tidal sandbank's surface (Middelkerke Bank, southern North Sea). Mar Geol 121:23–41

Howarth MJ (1982) Tidal currents of the continental shelf. In: Stride AH (ed) Offshore tidal sands: processes and deposits. Chapman & Hall, New York

Howarth MJ, Huthnance JM (1984) Tidal and residual currents around a Norfolk sandbank. Estuarine Coast Shelf Sci 19:105–117

Hulscher SJMH (1996) Tidal-induced large-scale regular bedform patterns in a three-dimensional shallow water model. J Geophys Res 101(C9):20727–20744

Hülsemann J (1955) Grossrippeln und Schrägsrichtungengs-Gefüge im Nordsee Watt un in der Molasse. Senck Leth 36:359–388

Huthnance JM (1973) Tidal current asymmetries over the Norfolk sandbanks. Estuarine Coast Mar Sci 1:89–99

Huthnance JM (1982a) On one mechanism forming linear sand banks. Estuarine Coast Mar Sci 14:79–99

Huthnance JM (1982b) On the formation of sand banks of finite extent. Estuarine Coast Mar Sci 15:277–299

James NP (1997) The cool-water carbonate depositional realm. In: James NP, Clarke JAD (eds) Cool-water carbonates. SEPM Spec Publ 56:1–20

Jin JH, Chough SK (2002) Erosional shelf ridges in the mid-eastern Yellow Sea. Geo-Mar Lett 21:219–225

Johnson HD (1977) Shallow marine sand bar sequences; an example from the late Precambrian of North Norway. Sedimentology 24:245–270

Johnson MA, Kenyon NH, Belderson RH, Stride AH (1982) Sand transport. In: Stride AH (ed) Offshore tidal sands, processes and deposits. Chapman & Hall, London

Jung WY, Suk BC, Min GH, Lee YK (1998) Sedimentary structure and origin of a mud-cored pseudo-tidal sand ridge, eastern Yellow Sea, Korea. Mar Geol 151:73–88

Kamp PJJ, Harmsen FJ, Nelson CS, Boyle SF (1988) Barnacle-dominated limestone with giant cross-beds in a non-tropical, tide-swept, Pliocene forearc seaway, Hawke's Bay, New Zealand. Sediment Geol 60:173–195

Kenyon NH, Stride AH (1970) The tide-swept continental shelf sediments between the Shetland isles and France. Sedimentology 14:159–173

Kenyon NH, Belderson RH, Stride AH, Johnson MA (1981) Offshore tidal sand banks as indicators of net sand transport and as potential deposits. In: Nio SD, Schuttenhelm RTE, Van Weering TjCE (eds) Holocene marine sedimentation in the North Sea basin. IAS Spec Publ 5:257–268

Laban C, Schuttenhelm RTE (1981) Some new evidence on the origin of the Zealand Ridges. In: Nio SD, Schuttenhelm RTE, Van Weering TjCE (eds) Holocene marine sedimentation in the North Sea basin. IAS Spec Publ 5:239–245

Lanckneus J, De Moor G, Stolk A (1994) Environmental setting, morphology and volumetric evolution of the Middelkerke Bank (southern North Sea). Mar Geol 121:1–21

Lanier WP, Feldman HR, Archer AW (1993) Tidal sedimentation from a fluvial to estuarine transition, Douglas Group, Missourian-Virgilian, Kansas. J Sediment Petrol 63:860–873

Lapierre F (1975) Contribution a l'etude geologique et sedimentologique de la Manche orientale. Philos Trans R Soc Lond A 1975:177–187

Le Bot S, Trentesaux A (2004) Types of internal structure and external morphology of submarine dunes under the influence of tide and wind-driven processes (Dover Strait, northern France). Mar Geol 211:143–168

Legg S, Adcroft A (2003) Internal wave breaking at concave and convex continental slopes. J Phys Ocean 33:2224–2246

Lesueur J-L, Rubino J-L, Giraudmaillet M (1988) Organisation et structures internes des dépots tidaux du Miocène rhodanien. Bull Soc Geol France 6:49–65

Levell BK (1980) A Late Precambrian tidal shelf deposit, the lower Sandfjord Formation, Finnmark, North Norway. Sedimentology 27:539–557

Liu ZX, Xia DX, Berné S, Yang WK, Marsset T, Tang YX, Bourillet J-F (1998) Tidal depositional systems of China's continental shelf, with special reference to the eastern Bohai Sea. Mar Geol 145:225–268

Liu Z, Berné S, Saito Y, Yu H, Trentesaux A, Uehara K, Yin P, Liu JP, Li C, Hu G, Wang X (2007) Internal architecture and mobility of tidal sand ridges in the East China Sea. Cont Shelf Res 27:1820–1834

Longhitano SG, Nemec W (2005) Statistical analysis of bed-thickness variation in a Tortonian succession of biocalcarenitic tidal dunes, Amantea Basin, Calabria, southern Italy. Sediment Geol 179:195–224

MacEachern JA, Bann KL, Pemberton SG, Gingras MK (2005) The ichnofacies paradigm: high-resolution paleoenvironmental interpretation of the rock record. In: MacEachern JA, Bann KL, Gingras MK, Pemberton SG (eds) Applied ichnology. SEPM Short Course Notes 52:27–64

Malikides M, Harris PT, Jenkins C, Keene J (1988) Carbonate sandwaves in the Bass Strait. Aust J Earth Sci 35:303–311

Martel AT, Allen PA, Slingerland R (1994) Use of tidal-circulation modeling in paleogeographical studies; an example from the Tertiary of the Alpine perimeter. Geology 22:925–928

McCave IN (1971) Sandwaves in the North Sea off the coast of Holland. Mar Geol 10:199–225

McCave IN, Langhorne DN (1982) Sand waves and sediment transport around the end of a tidal sand bank. Sedimentology 29:95–110

Mellere D, Steel R (1995) Facies architecture and sequentiality of nearshore and "shelf" sandbodies; Haystack Mountains Formation, Wyoming, USA. Sedimentology 42:551–574

Mellere D, Steel RJ (1996) Tidal sedimentation in the Inner Hebrides half grabens, Scotland: the Mid-Jurassic Bearreraig Sandstone Formation. In: de Batist M, Jacobs P (eds) Geology of siliciclastic shelf seas. Geol Soc Lond Spec Publ 117:49–79

M'Hammdi N, Berné S, Bourillet J-F, Auffret J-P (1992) Architecture of a tidal sand bank; the Sark Bank (Channel Islands). In: Flemming BW (ed) Modern and ancient clastic tidal deposits. Courier Forschunginstitut Senckenberg 151:59–60

Mitchell AJ, Ulicny D, Hampson GJ, Allison PA, Gorman GJ, Piggott MD, Wells MR, Pain CC (2010) Modeling tidal current-induced bed shear stress and palaeocirculation in an epicontinental seaway: the Bohemian Cretaceous Basin, Central Europe. Sedimentology 57:359–388

Mutti E, Rosell J, Allen GP, Fonnesu F, Sgavetti M (1985) The Eocene Baronia tide dominated delta-shelf system in the Ager Basin. In: Mila MD, Rosell J (eds) Excursion guidebook, 6th IAS European regional meeting, Lleida, pp 579–600

Nio SD, Yang C (1991) Diagnostic attributes of clastic tidal deposits: a review. In: Smith DG, Reinson GE, Zaitlin BA, Rahmani RA (eds) Clastic tidal sedimentology. Can Soc Petrol Geol Mem 16:3–28

Nelson CS, Winefield PR, Hood SD, Caron V, Pallentin A, Kamp PJJ (2003) Pliocene Te Aute limestones, New Zealand; expanding concepts for cool-water shelf carbonates. NZ J Geol Geophys 46:407–424

Off T (1963) Rythmic linear sandbodies caused by tidal currents. AAPG Bull 47:324–341

Pan S, MacDonald N, Williams J, O'Connor BA, Nicholson J, Davies AM (2007) Modelling the hydrodynamics of offshore sandbanks. Cont Shelf Res 27:1264–1286

Pantin HM, Evans CDR (1984) The Quaternary history of the central and southwestern Celtic Sea. Mar Geol 57:259–293

Park SC, Lee BH, Yoo DG, Lee CW (2006) Late Quaternary stratigraphy and development of tidal sand ridges in the eastern Yellow Sea. J Sed Res 76:1093–1105

Pattiaratchi C, Collins M (1987) Mechanisms for linear sandbank formation and maintenance in relation to dynamical oceanographic observations. Prog Oceanograph 19:117–176

Pingree RD, Griffiths DK (1979) Sand transport paths around the British Isles resulting from M (sub 2) and M (sub 4) tidal interactions. J Mar Biol Assoc UK 59:497–513

Pingree RD, Maddock L (1979) The tidal physics of headland flows and offshore tidal bank formation. Mar Geol 32: 269–289

Posamentier HW (2002) Ancient shelf ridges—a potentially significant component of the transgressive systems tract: case study from offshore northwest java. Am Assoc Petrol Geol Bull 86:75–106

Pratt LJ (1990) The physical oceanography of sea straits. Kluwer, Dordrecht

Proctor R, Carter L (1989) Tidal and sedimentary response to the late Quaternary closure and opening of Cook Strait, New Zealand; results from numerical modeling. Paleoceanography 4:167–180

Pugh DT (1987) Tides, surges and mean sea-level; a handbook for engineers and scientists. Wiley, Chichester

Ramaswamy V, Rao PS, Rao KH, Thwin S, Roa NS, Raiker V (2004) Tidal influence on suspended sediment distribution and dispersal in the northern Andaman Sea and Gulf of Martaban. Mar Geol 208:33–42

Rao PS, Ramaswamy V, Thwin S (2005) Sediment texture, distribution and transport on the Ayeyarwady continental shelf, Andaman Sea. Mar Geol 216:239–247

Reesink AJH, Bridge JS (2007) Influence of superimposed bedforms and flow unsteadiness on the formation of cross strata in dunes and unit bars. Sediment Geol 202:281–296

Reesink AJH, Bridge JS (2009) Influence of superimposed bedforms and flow unsteadiness on the formation of cross strata in dunes and unit bars - Part 2, further experiments. Sediment Geol 222:274–300

Reynaud JY, Tessier B, Berné S, Chamley H, De Batist M (1999a) Tide and wave dynamics on a sand bank from the deep shelf of the Western Channel Approaches. Mar Geol 161:339–359

Reynaud JY, Tessier B, Proust JN, Dalrymple RW, Marsset T, De Batist M, Bourillet J-F, Lericolais G (1999b) Eustatic and hydrodynamic controls on the architecture of a deep shelf sand bank (Celtic Sea). Sedimentology 46:703–721

Reynaud JY, Rage A, Tessier B, Néraudeau D, Bracini E, Carriol R-P, Clet-Pellerin M, Moullade M, Lericolais G (1999c) Importations et remaniements de faunes dans les sables de la plate-forme profonde des Approches Occidentales de la Manche. Oceanol Acta 22:381–396

Reynaud JY, Tessier B, Auffret J-P, Berné S, De Batist M, Marsset T, Walker P (2003) The offshore sedimentary cover of the English Channel and its northern and western approaches. J Quart Sci 18:261–282

Reynaud JY, Dalrymple RW, Vennin E, Parize O, Besson D, Rubino J-L (2006) Topographic controls on producing and depositing tidal cool-water carbonates, Uzès basin, SE France. J Sediment Res 76:117–130

Rubin DM (1987) Cross-bedding, bedforms and paleocurrents, vol 1, Concepts in Sedimentology and Paleontology. SEPM, Tulsa

Rubin DM, Hunter RE (1987) Bedform alignment in directionally varying flows. Science 237:276–278

Rubin DM, Ikeda H (1990) Flume experiments on the alignment of transverse, oblique, and longitudinal dunes in directionally varying flows. Sedimentology 37:673–684

Rubin DM, McCulloch DS (1980) Single and superimposed bedforms: a synthesis of San Francisco bay and flume observations. Sediment Geol 26:207–231

Shaw J, Amos CL, Greenberg DA, O'Reilly CT, Parrott DR, Patton E (2010) Catastrophic tidal expansion in the Bay of Fundy, Canada. Can J Earth Sci 47:1079–1091

Seilacher A (1967) Bathymetry of trace fossils. Mar Geol 5:413–428

Sinha B, Pingree RD (1997) The principal lunar semidiurnal tide and its harmonics: baseline solutions for M2 and M4 constituents on the North-West European continental shelf. Cont Shelf Res 17:1321–1365

Snedden JW, Dalrymple RW (1999) Modern shelf sand ridges: from historical perspective to a unified hydrodynamic and evolutionary model. In: Bergman KM, Snedden JW (eds) Isolated shallow marine sand bodies: sequence stratigraphic analysis and sedimentological perspectives. SEPM Spec Publ 64:13–28

Southard JB, Boguchwal LA (1990) Bed configurations in steady unidirectional water flows. Part 2. Synthesis of flume data. J Sediment Petrol 60:649–657

Stride AH (1963) Current-swept sea floors near the southern half of Great Britain. Quart J Geol Soc Lond 119:175–199

Stride AH (ed) (1982) Offshore tidal sands: processes and deposits. Chapman & Hall, London, 222 p

Stride AH, Belderson RH, Kenyon NH, Johnson MA (1982) Offshore tidal deposits: sand sheet and sand bank facies. In: Stride AH (ed) Offshore tidal sands: processes and deposits. Chapman & Hall, London

Surlyk F, Noe-Nygaard N (1991) Sand bank and dune facies architecture of a wide intracratonic seaway; Late Jurassic-Early Cretaceous Raukelv Formation, Jameson Land, East Greenland. In: Miall AD, Tyler N (eds) The three-dimensional facies architecture of terrigenous clastic sediments and its implications for hydrocarbon discovery and recovery. Concepts in Sediment Paleo 3:261–276

Suter JR (2006) Facies models revisited: clastic shelves. In: Posamentier HW, Walker RG (eds) Facies models revisited. SEPM Spec Publ 84:339–397

Swift DJP (1975) Tidal sand ridges and shoal retreat massifs. Mar Geol 18:105–134

Sztano O, De Boer P (1995) Basin dimensions and morphology as controls on amplification of tidal motions (the early Miocene North Hungarian Bay). Sedimentology 42:665–682

Tillman RW, Martinsen RS (1984) The Shannon shelf ridge sandstone complex, Salt Creek Anticline area, Powder River basin, Wyoming. In: Tillman RW, Siemers CT (eds) Siliciclastic shelf sediments. SEPM Spec Publ 34:1–34

Trentesaux A, Stolk A, Berné S (1999) Sedimentology and stratigraphy of a tidal sand bank in the southern North Sea. Mar Geol 159:253–272

Uehara K, Scourse JD, Horsburgh KJ, Lambeck K, Purcell AP (2006) Tidal evolution of the northwest European shelf seas from the last glacial maximum to the present. J Geophys Res 111:C09025

Vail PR, Mitchum RM, Thomson S (1977) Seismic stratigraphy and global changes of sea level; Part 4, Global cycles of relative changes of sea level. In: Payton CE (ed) Seismic stratigraphy; Applications to hydrocarbon exploration. AAPG Memoir 26:83–97

Van der Molen J, Gerrits J, De Swart HE (2004) Modelling the morphodynamics of a tidal shelf sea. Cont Shelf Res 24:483–507

Van Rijn LC (1982) Prediction of bed forms, alluvial roughness and sediment transport. Delft Hydraulics, S 487–11, Delft, The Netherlands

Van Veen J (1936) Onderzoekingen in de Hoofden. Algemene Landsdruckerij's Gravenhage, 252 p

Viana AR, Faugères J-C, Stow DAV (1998) Bottom current controlled sand deposits—a review of modern shallow to deep-water environments. Sediment Geol 115:53–80

Visser MJ (1980) Neap-spring cycles reflected in Holocene subtidal large-scale bedform deposits: a preliminary note. Geology 8:543–546

Walker RG, Bergman KM (1993) Shannon sandstone in Wyoming: a shelf ridge complex reinterpreted as lowstand shoreface deposits. J Sediment Petrol 63:839–851

Wells MR, Allison PA, Piggott MD, Gorman GJ, Hampson GJ, Pain CC, Fang F (2007) Numerical modeling of tides in the late Pennsylvanian Midcontinent seaway of North America with implications for hydrography and sedimentation. J Sediment Res 77:843–865

Wells MR, Allison PA, Piggott MD, Hampson GJ, Pain CC, Gorman GJ (2010) Tidal modeling of an ancient tide-dominated seaway, part 2: the Aptian Lower Greensand seaway of Northwest Europe. J Sediment Res 80: 411–439

Wilson JB (1982) Shelly faunas associated with temperate offshore tidal deposits. In: Stride AH (ed) Offshore tidal sands: processes and deposits. Chapman & Hall, London

Wilson JB (1988) A model for temporal changes in the faunal composition of shell gravels during a transgression on the continental shelf around the British Isles. In: Nelson CS (ed) Non-tropical shelf carbonates; modern and ancient. Sed Geol 60:95–105

Wright J, Colling A, Park D (Open University S330 Course readers) (1999) Waves, tides and shallow-water processes, 2nd edn. Butterworth-Heinemann in association with the Open University, Oxford

Yalin MS (1964) Geometrical properties of sand waves. Proc Am Soc Civil Eng 90:105–119

Yang ZS, Liu JP (2007) A unique Yellow River-derived distal subaqueous delta in the Yellow Sea. Mar Geol 240:169–176

Yoshida S, Johnson HD, Pye K, Dixon RJ (2004) Transgressive changes from tidal estuarine to marine embayment depositional systems: the Lower Cretaceous Woburns Sands of southern England and comparison with Holocene analogs. AAPG Bull 88:1433–1460

Yoshida S, Steel RJ, Dalrymple RW (2007) Changes in depositional processes - an ingredient in the generation of new sequence-stratigraphic models. J Sediment Res 77:447–460

Zimmerman JTF (1978) Topographic generation of residual circulation by oscillatory (tidal) currents. Geophys Astrophys Fluid Dyn 11:35–47